Abstract

A NOVEL NUCLEOLAR LOCALIZATION OF A SYNAPTOPODIN-2 ISOFORM IN PROLIFERATING HT29 CELLS

By Sarah Urankar

July 2021

Directors of Thesis: Dr. Jean Luc Scemama & Dr. Margit Schmidt

DEPARTMENT OF BIOLOGY

EAST CAROLINA UNIVERSITY

Members of the Synaptopodin family regulate α-actinin and actin-bundling activity, in an isoform specific manner (Asunama et al., 2005). The ability to affect actin polymerization and bundling highlights the critical role that synaptopodin members play in normal and pathologic cells. Synaptopodin-2 (Synpo2) is one member of the synaptopodin family that is capable of inducing actin polymerization (Chalovich & Schroeter, 2010), suggesting an important role in cell migration, adhesion, division, and development. Synpo2 has also been described as a valuable biomarker for several invasive cancers due to its ability to alter cell motility in response to external stimuli (Kai et al, 2015). Although most data support the Synpo2's role as a tumor suppressor (Xia et al., 2018; Liu, et al., 2018; Kai et al, 2012; Cebrian et al., 2008; Sanchez-Carbayo et al., 2003; Jing et al., 2004; Lin et al., 2001), it has been reported that under certain conditions, the loss of Synpo2 expression led to decreased motility and invasiveness (De Ganck et al, 2009). These contradictory reports of the influence of the expression of Synpo2 in cell migration and tumor stimulation/suppression demonstrate the need for

further research. Synpo2 exists as five isoforms, which are the result of alternative splicing and cause differences at the N-terminal end of the proteins (Chalovich & Schroeter, 2010). Each isoform has a unique response to different chemokinetic stimuli (Kai et al., 2012). To improve the understanding of individual roles that these isoforms play in human colorectal cancer cells, this study considers the difference in expression of specific Synpo2 isoforms in HT29 cells. We observed intense and irregular staining in areas within the nucleus, with a pattern that was 90% correlated with markers of nucleoli. Furthermore, transcriptional inhibition resulted in a loss of nuclear stain. Induction of differentiation in HT29 cells with sodium butyrate, resulted in a loss of nuclear expression detected by the synaptopodin 2 antibody, but showed an increase in previously undetected cytoplasmic expression. RT-PCR and Western blot analysis showed that HT29 cells lacked Synpo2 isoform B, but expressed its smaller truncated isoform, myopodin. Nuclear fractions detected the expression of a smaller cross-reactive protein at approximately 55 kDa. This unexpected protein recognized by our affinity purified antibody could potentially be a previously uncharacterized Synpo2 isoform. The nucleolar expression detected though immunofluorescence suggests a highly critical role in normal cell function.

NOVEL NUCLEOLAR LOCALIZATION OF SYNAPTOPODIN-2 ISOFORM IN PROLIFERATING HT-29 CELLS

A Thesis

Presented to the Department of Biology

EAST CAROLINA UNIVERSITY

In Partial Fulfillment of the Requirements for the Degree

Master of Science in Molecular Biology and Biotechnology

Sarah E. Urankar

July 2021

NOVEL NUCLEOLAR LOCALIZATION OF SYNAPTOPODIN-2 ISOFORM IN PROLIFERATING HT-29 CELLS

By

Sarah Urankar

APPROVED BY:

DIRECTOR OF THESIS: _____
Jean Luc Scemama, PhD

COMMITTEE MEMBER: _____
Margit Schmidt, PhD

COMMITTEE MEMBER: _____
Joseph Chalovich, PhD

COMMITTEE MEMBER: _____
John Stiller, PhD

CHAIR OF THE DEPARTMENT
OF BIOLOGY: _____
David Chalcraft, PhD

DEAN OF THE
GRADUATE SCHOOL: _____
Paul Gemperline, PhD

ACKNOWLEDGEMENTS

I have to start by thanking my incredibly patient and supportive mentors, Dr. Jean-Luc Scemama, Dr. Margit Schmidt and Dr. Joseph Chalovich. Dr. Scemama has gone above and beyond what any mentor/teacher is expected to do for a student and for that I will be forever grateful. He has shown me, over and over again, how to be an effective teacher as well as a loyal friend. I want to thank him for never giving up on me even when it seemed like I had given up on myself. I am also especially thankful to Dr. Schmidt for pushing me to solve problems, teaching me to learn from mistakes, and helping me acquire the necessary skills to be successful in a professional research laboratory setting. She has taught me what it means to work hard and I am a better person and scientist from having learned from her. I would also like to thank my final committee member, Dr. Joseph Chalovich, for allowing me to use his laboratory and resources to complete my project. With the continued support from my amazing committee, I have been allowed a unique opportunity to overcome obstacles that many students do not face. I would also like to extend a special thanks to Dr. John Stiller, for advocating on my behalf to the Graduate Council Executive Committee to help make all of this possible.

My appreciation is also extended to my lab mates and other technicians who offered support throughout my time at East Carolina. Lucy Conaty, Daniel White and Kelli Shortt helped me weather the storm of failed experiments, confusing data and general frustrations that come with being a graduate student. I would also like to thank Tammy Baxley for taking time out of her day to teach me in a judgement free-zone. Making mistakes is a part of learning (especially in a lab!) but being able to do so in a

way that is encouraging, instead of discouraging, is critical for maintaining a desire to push through. This is the kind of support I found within my fellow lab mates and technicians, and for that support I am truly thankful.

Finally, I would like to thank my family, who has sacrificed their time in order for me to succeed. Thank you all for your support, encouragement, and understanding while I focused all my attention on academics. Especially to my husband, Tony, who kept me grounded when I felt like things were spiraling out of control. Your continued faith in me is a constant reminder of why I was willing to run off to England with you all those years ago.

TABLE OF CONTENTS

LIST OF TABLES

APPENDIX A- Tables

LIST OF FIGURES

LIST OF SYMBOLS AND ABBREVIATIONS

µg - micrograms

µL - microliter

mL - milliliter

ABPs - Actin-binding proteins

BSA - Bovine serum albumin

DAPI - 4',6-diamidino-2-phenylindole

DMEM/F-12 - Dulbecco's Modified Eagle Medium/Nutrient Mixture F-12

F-actin - Filamentous actin

G-actin - Globular actin

Myo - Myopodin

PBS - phosphate-buffered saline

SDS - sodium dodecyl sulfate

Synpo2 - Synaptopodin-2

CHAPTER 1: INTRODUCTION

SECTION 1-1: The synaptopodin family

There are three members of the synaptopodin family that have been described: synaptopodin, synaptopodin-2, and synaptopodin-2-like. Synaptopodin, the founding member of the family, was first discovered in kidney podocytes and postsynaptic densities of telencephalic synapses (Mundel et al., 1997). Synaptopodin-2 (Synpo2), also referred to as fesselin or myopodin, was discovered in avian smooth muscle (Leinweber et al., 1999), and later described in heart and skeletal muscle and is thought to be involved in cytoskeletal organization (Weins et al., 2001). Synaptopodin-2-like, also known as tritopodin (Claeys et al., 2009) or CHAP (Beqqali, 2010), is similar to synaptopodin-2 in that it is found in the heart and skeletal muscle tissue and functions to stabilize sarcomeres.

Each of the three family members have their own isoforms that are produced by alternative splicing (De Ganck et al., 2008; Chalovich and Schroeter, 2010). An important and defining characteristic of the synaptopodin family is that each protein is basic and has a high proline content. Being rich in proline, prevents these proteins from forming any secondary or tertiary structures under normal physiological conditions (Khaymina et al., 2007). Therefore, synaptopodin family members are capable of acting as a hub protein, interacting with other proteins. One common characteristic of the synaptopodin family members is its ability to bind actin and several actin associating proteins (Asanuma et al., 2005; Yu & Luo, 2006; Schroeter & Chalovich, 2004; Kołakowski et al., 2004). This thesis focuses on synaptopodin-2, which has been shown to not only bind actin, but also to stimulate its polymerization and bundle actin filaments (Beall & Chalovich, 2001).

SECTION 1-2: Introduction to Synaptopodin-2 and its isoforms

Five different isoforms of Synpo2 have been described as a product of alternative splicing (Chalovich & Schroeter, 2010). With the exception of myopodin, and the smallest unnamed isoform, each of the synaptopodin-2 transcript variants includes exon 1, 2, 3, and the complete 4a (Figure 1). The mRNA transcript variants 1, 2, and 3 include either exons 6, 4b or 5 and encodes a 1261, 1093 or 1109 amino acids long protein, respectively known as isoform A, isoform B, and isoform C (Chalovich & Schroeter, 2010). The smallest synaptopodin-2 isoform is unnamed and only includes exons 1, 2 and a small portion of exon 6. Myopodin is the smallest named synaptopodin-2 isoforms, which is 698 amino acids long and only includes 689 of the 794 amino acids of exon 4a and all nine of the amino acids of exon 4b (Chalovich & Schroeter, 2010). In addition to the PDZ domain which is located at the N-terminal of the longer isoforms, the nine amino acids that form the 4b exon are present in isoform B and myopodin, are located at the C-terminal end of these variants and have been shown to contribute to Synpo2's ability to respond to chemokinetic stimuli in certain prostate cancer cells (Kai et al., 2012).

Several previous studies regarding synaptopodin-2 have used the name myopodin to describe all isoforms of synaptopodin-2 (De Ganck et al., 2008; Weins et al., 2001; Kai et al., 2012; Lin et al., 2001; Cebrian et al., 2008). In the literature review, we will conserve their nomenclature; however, to avoid confusion, in this thesis we will refer to myopodin as the shortest named isoform as described by Schroeter and Chalovich (2010). The other isoforms will be referred to as synaptopodin-2 isoform A, B or C.

Figure 1: Synaptopodin-2 Isoforms

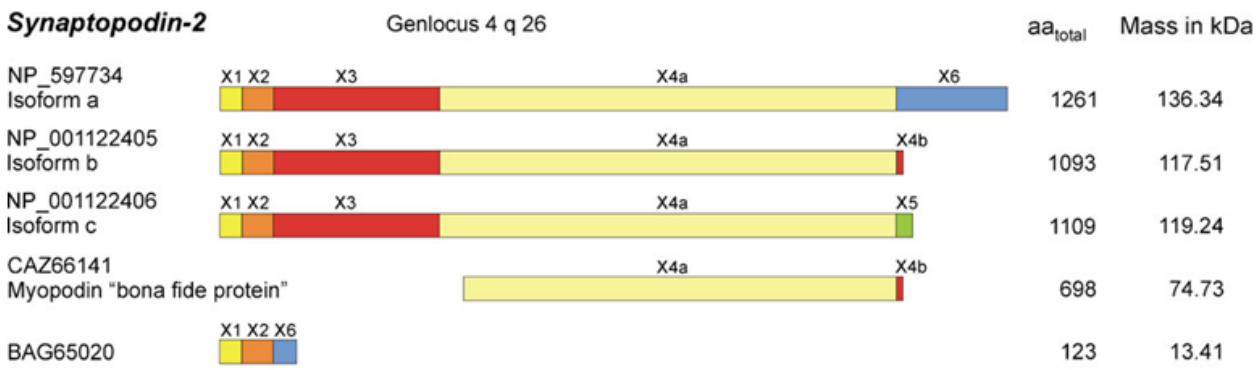

Figure 1: Synaptopodin-2 isoforms as a result of alternative splicing (Chalovich & Schroeter, 2010).

Mammalian myopodin was first characterized as a novel actin-bundling protein (Weins et al., 2001) and later shown to be a product of alternative splicing of synaptopodin-2 (Schroeter et al., 2008). Previously to this, it had been shown that partial or complete deletions of myopodin and its epigenetic silencing through hypermethylation correlated to the invasiveness of prostate and bladder cancers, respectively (Lin et al., 2001; Cebrian et al., 2008). The primers used in these studies were non-isoforms specific (annealing in the region between exon 1 and 4a), and therefore, were not amplifying myopodin but instead all the synaptopodin-2 splice variants. Nevertheless, down-regulating the expression of synaptopodin-2 has been associated with increased invasiveness and motility in human prostate (PC-3), bladder (RT4), and breast (MDA-MB-231, BT-549, SK-BR-3, MDA-MB-468, BT-474, T-47D, MCF-7, MDA-MB-453, MDA-MB-436, and MCF10A) cancer cell lines (De Ganck et al., 2008; Cebrian et al., 2008; Xia et al., 2018). From these studies, the authors hypothesized that in normal cells, myopodin (Synpo2) acts as a tumor suppressor gene and its function is correlated with its nuclear location. Further studies that analyzed the localization of myopodin in normal urothelium and bladder cancer, demonstrated that in the transformed tissue, Synpo2 translocates to the cytoplasm, where its association with the actin cytoskeleton is believed to play a role as a tumor promoter (De Ganck et al., 2009).

Previous studies have also shown that myopodin is localized in the nucleus of undifferentiated C2C12 cells, but upon differentiation translocates into the cytoplasm (Weins et al., 2001) which is in contradiction with its suggested tumor promoter role when expressed in the cytoplasm. Over-expression of a wild-type myopodin, in non-invasive mouse C2C12 myoblast cells promote invasion of these cells into a collagen matrix, while over-expression of truncated myopodin, which lack a nuclear export signal, do not induce invasiveness (Van Impe et al., 2003). These data demonstrate that the translocation of myopodin between the nuclear and cytoplasmic compartment is essential to regulate its activity. These contradictory results

demonstrate that more studies are needed in order to understand the role of synaptopodin-2 in normal and transformed cells. It is important to indicate that the above studies did not investigate the roles of individual isoforms of Synpo2. A possible explanation for the contrasting results obtained could be that the various isoforms may be differentially expressed in normal and transformed cells, or alternatively, the isoforms may function differently from one another.

Figure 2: Synaptopodin-2 Localization in Normal and Cancerous cells

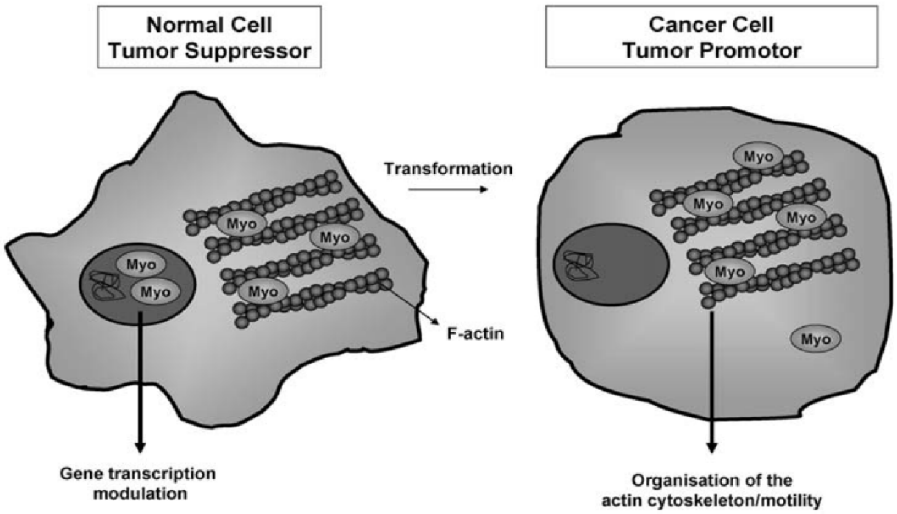

Figure 2: Diagram of Synaptopodin-2 (myopodin) localization and suggested function in normal and cancerous cells. Myo, myopdin (De Ganck et al., 2009).

SECTION 1-3: Binding Partners of Synaptopodin-2

Each member of the synaptopodin family (synaptopodin, synaptopodin-2, and synaptopodin 2-like) are proline rich basic proteins, preventing the formation of globular domains (Mundel et al, 1997). Synaptopodin-2 has also been shown to act as a hub protein (Khaymina et al., 2007); allowing it to bind to multiple binding partners. Hub proteins have received a significant amount of attention in recent years because of their capability to form numerous physical interactions; their role is essential in mediating several cellular processes, which could serve as a potential therapeutic value.

Fesselin was described by Schroeter et al. as the avian homolog of mammalian synaptopodin-2 (2008). Fesselin is an actin binding protein (Leinweber et al., 1999) that stimulates actin nucleation and polymerization. Synaptopodin-2 binds both F and G-actin, and causes rapid polymerization of G-actin into F-actin, when compared to unbound G-actin (Beall & Chalovich, 2001). The formation of nucleation centers occurs at a ratio of 3 actin monomers to 1 synaptopodin-2 protein (Figure 3). Schroeter and Chalovich found nucleation center formation is regulated by the concentration of calcium-calmodulin (2004). Although in the presence of calcium-calmodulin, the binding of fesselin to F-actin and its ability to bundle F-actin is unaffected, fesselin's stimulatory effect on G-actin polymerization was significantly reduced, suggesting that fesselin has a major role as an actin-polymerizing factor (Schroeter and Chalovich, 2004).

The assembly of G-actin into F-actin is a major contributing factor to the cell cytoskeleton architecture and as such plays a crucial role in many cell functions from movement and organelle distribution to the regulation of gene expression. Actin filaments are extremely dynamic structures whose state of assembly is largely dependent on actin-binding proteins (ABPs). Since actin polymerization rates have such a crucial role in the reorganization of the cell cytoskeleton and the cell cycle, ABPs capable of altering actin polymerization rates are also

responsible for mediating these processes (Lodish et al., 2000). These data suggest that Synpo2 may regulate important cellular functions, such as cell cycle progression and cell motility. Aside from actin, several additional proteins, such as myosin, calmodulin, α-actinin and zyxin have been shown to associate with synaptopodin-2 (Asanuma et al., 2005; Pham & Chalovich, 2006; Yu & Luo, 2006; Shen et al., 2005). Multiple interactions are thought to be possible because Synpo2 lacks any real secondary and tertiary structures in its native state (Khaymina et al., 2007). Synaptopodin-2 has been shown to co-localize with α-actinin (Linnemann et al., 2010). Previous research suggests that members of the synaptopodin family associate with specific α-actinin isoforms to promote the polymerization of actin (Asanuma et al., 2005). Association with α-actinin-4, an isoform of α-actinin that has been shown to shuttle from the cytoplasm to the nucleus during actin depolymerization (Honda et al., 1998), has been linked with the translocation of synaptopodin-2 from the cytoplasm to the nucleus, where it induces actin bundling (Weins et al., 2001). Association with cell cytoskeleton proteins suggest Synpo2 might be involved with the chromatin-remodeling complex, and therefore, may be an important regulator of transcriptional activity and cell cycle progression (Castano et al., 2010).

Figure 3: Synaptopodin-2 stimulates actin polymerization

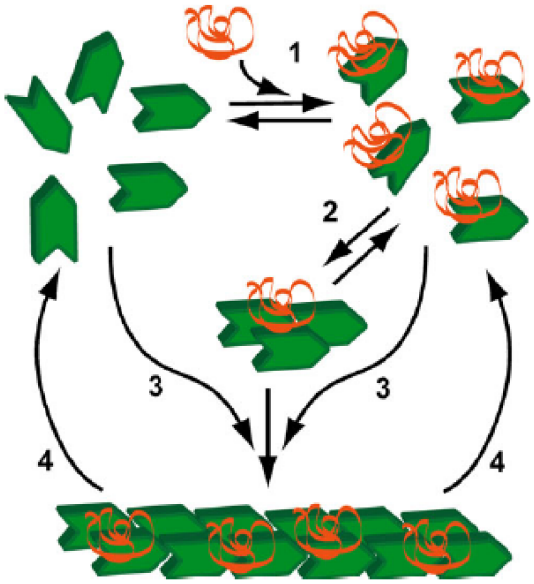

Figure 3: Schematic representation of the proposed effect synaptopodin-2 has on actin polymerization. Actin (green) binds to synaptopodin-2 (orange) to form a complex at a 3:1 ratio (Chalovich & Schroeter, 2010).

SECTION 1-4: Cell Cycle

The integrity of the cell's genetic material is dependent on the ability of the cell to monitor DNA replication processes until completion or block the transition of one phase of the cell cycle to the next if any problem is detected (Cooper, 2000). There are four distinct phases of the cell cycle: the G1 phase, S phase, and G2 phase, which are collectively known as interphase and the M phase (Figure 4). During the G1 phase, cells increase in size and prepare for DNA synthesis which begins when cells enter the S phase. The gap between DNA synthesis and mitosis is known as G2. During G2 the cells will continue to grow until they are ready to undergo mitosis (M phase). When cells reach M phase, cell growth will arrest and the cell divides into two daughter cells (Cooper, 2000). The transitions between the phases of the cell cycle are unidirectional and highly coordinated. Checkpoints in the cell cycle, working through signal transduction pathways, regulate the cell cycle in response to cell stress or other factors. For example, DNA-damage will generate a signal causing cells to arrest in the G1 and G2 phases and will slow down DNA synthesis while transcription of repair genes is induced (Johnson and Rao, 1970).

The progression through the cell cycle is a highly ordered series of events that is critically dependent on several key regulatory proteins. Countless proteins within the cell undergo translocation, some type of modification, or vary in concentration in a cell-cycle dependent manner. It has been estimated that approximately 700 genes display transcriptional fluctuation that is consistent with cell-cycle progression (Cho et al. 2001). A wide variety of cytoskeletal reorganization genes are regulated in a cell-cycle dependent manner. Several genes that are involved in cell motility and the extracellular matrix are predominantly expressed in the M phase. Transcripts that are upregulated during S phase overlap with genes that are induced by DNA damage, which suggests that while a cell is synthesizing new DNA, it is also

constantly checking for and repairing damage to the newly synthesized DNA (Cho et al., 2001). Proliferating cells are continuously repeating the cell-cycle and are in a constant protein flux to meet the demands of the cell. Actively growing cells have a high demand for ribosomes, and as such, rely on the nucleolus to keep a steady supply, which will need to be synthesized each time the cell divides.

Figure 4: Normal Cell Cycle Progression

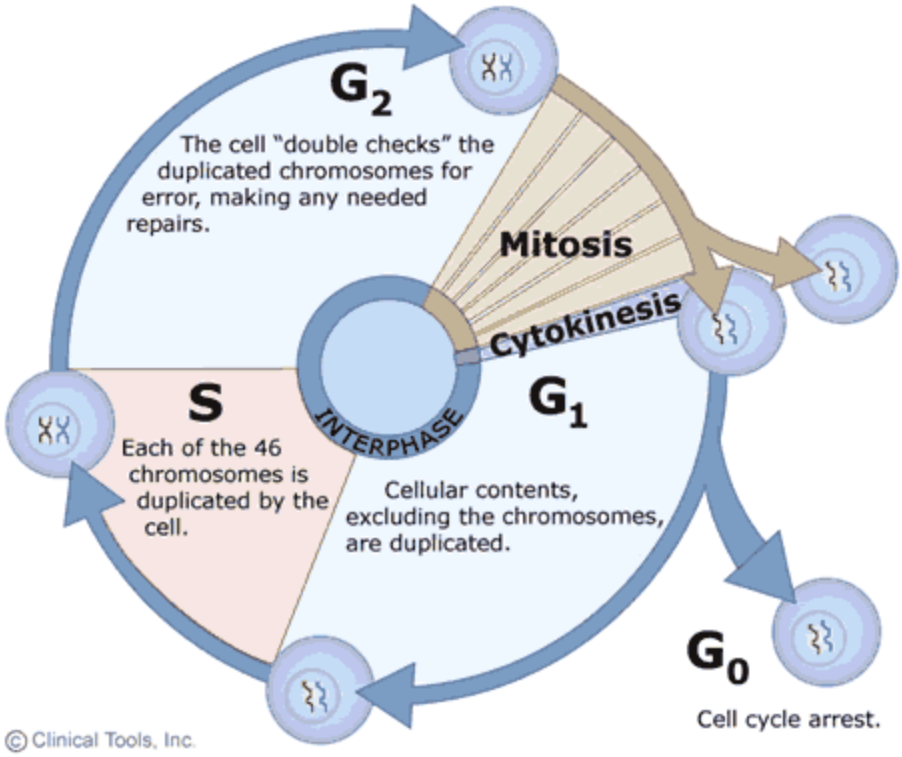

Figure 4: Schematic representation of a normal cell cycle (Scicurious, 2010).

SECTION 1-5: The Nucleolus

The nucleolus is the most prominent substructure located within the nucleus of the cell. The function of the nucleolus is intimately connected to cell growth, division, and proliferation. From the time the nucleolus was first described until recent years, the function of nucleoli has been predominately and almost exclusively associated with biogenesis of rRNA by RNA polymerase I (Busch & Smetana, 1970; Hadjiolov, 1985). Due to the elevated demand for protein synthesis in proliferating cells, it is estimated that rRNA synthesis accounts for approximately 50% of the total RNA production in an actively growing and dividing cell (Zylber & Penman, 1971).

The nucleolus is not bound by a membrane, but is organized around chromosomal regions, whose primary transcript of the rRNA genes is the large 45S pre-rRNA, which contains the 5.8S, the 18S, and the 28S rRNAs. There are three distinguishable regions within the nucleolus: the fibrillar center, the dense fibrillar component, and the granular component (Cooper, 2000). Each of the different regions have a specific role in rRNA gene transcription, processing, and the assembly of the ribosome, within the nucleoli. Transcription for the 18S, 5.8S and 28S rRNAs is driven by nucleolar RNA polymerase I and is located in the fibrillar centers, just at the boundary with the dense fibrillar component of the nucleoli (Cooper, 2000). The pre-rRNA is then processed in the dense fibrillar component and will continue to be processed in the granular component. The 5S rRNA is the fourth ribosomal RNA, which is independently transcribed as a precursor by RNA polymerase III, will assemble with the 5.8S and 28S RNAs to form the large 60S (Raska et al., 2004). Ribosomes are assembled in the granular component with ribosomal proteins to form pre-ribosomal subunits, ready to be exported into the cytoplasm.

Although rRNA has largely been the focus of nucleolar activity for many years, advances in microscopic techniques and large-scale proteomic studies have provided greater insight into

the structure and composition of the nucleolus, giving a broader understanding of its role within the cell. Today, the nucleolus is considered to be as diverse as the proteins that it is composed of. There are over 700 human proteins that have been identified as nucleolar and only an estimated 30% of them play a role in the biogenesis of ribosomes (Cho et al. 2001).

Aside from rRNA transcription, the highly organized nucleolus has a role in cellular functions affecting cell-cycle progression, stress responses, and has even been correlated to ageing (Tsai & McKay, 2002; Rubbi & Milner, 2003; Raska et al., 2006; Boulon et al., 2010). The distribution of the nucleolus has been shown through previous studies to mediate the stabilization of p53 proteins in response to DNA damage and other stresses to the cell (Boulon et al., 2010).

Though the nucleolus has been studied in great detail, there are still a significantly large number of uncharacterized/novel proteins that are yet to be described for their role within the nucleolus. Some of the most intriguing features of the nucleolus today are correlated to their expression in cancerous cells. It is understandable that cells that are continuously proliferating, such as cancerous cells, have a greater protein requirement than non-proliferating cells; therefore, the up-regulation in rRNA transcription often coincides with an increased size and/or number of nucleoli within the cell (Raska et al., 2006). Consequently, the nucleolus can be used as an important biomarker for cancer diagnosis and prognosis.

The architecture of the nucleolus, as with the rest of the nucleus, is extremely dynamic and dependent on the physiological state of the cell. At the end of G2, as the cells enter mitosis the nuclear envelope begins to deteriorate and most of transcriptional activity ceases and the nucleolus is broken down and is then reassembled at the beginning of G1 at the onset of rRNA transcription (Cooper, 2000). The disassembly and reassembly of the nuclear envelope during the different phases of the cell cycle is correlated to a continuous flux, in activity and location, of nearly all nuclear proteins (Rubbi & Milner, 2003; Raska et al., 2006).

Fluctuation in several nucleolar components is correlated with transcription levels. As transcription is inhibited, the relative levels of nucleolar components often increases or decreases in quantity and rarely remains constant (Anderson, 2005). If the quantity of nucleolar components is unaffected by altered transcription levels, frequently their subcellular localization will be affected. Understanding nucleolar protein expression patterns can be another useful tool in identifying cancer progression.

SECTION 1-6: Colorectal Cancer

In the United States, cancer is the second leading cause of death (Siegel et al., 2020). Despite an overall decline in cancer related deaths over the past 30 years, colorectal cancer is still the second leading cause of cancer death in the United States for men and women (Siegel et al., 2020). Two factors have been shown to dramatically increase the risk of developing colorectal cancers; family history and age (Siegel et al., 2020).

Colorectal cancer normally progresses through a series of stages, Stages I-IV. During Stage 0, abnormal cells are formed in the mucosa of the colon. In Stage 1, the cells in the mucosa can be either cancerous or precancerous and begin to spread to the submucosa and the lower tissue layers. At Stage IIA, the cancer has spread through the muscle and reached the serosa. When cells reach Stage IIB, the cancer has breached the serosa, but has not yet metastasized to other organs. Upon reaching Stage IIC the cancer spreads to other nearby organs. Classifying Stage III cancer is dependent upon the extent of invasion from the origin and by the number of lymph nodes the cancer has spread to. At Stage IV, the cancer has metastasized to major organs that are not locally near the abdominal wall or colon (American Cancer Society, 2020). The progression through these stages results in the alteration of gene expression, such as activating oncogenes or inactivating tumor suppressor genes (Bevan & Rutter, 2018). Determining the level of expression of Synpo2, and its isoforms, in proliferating

and colorectal cancer cells will contribute to understanding the role that Synpo2 has on the invasiveness of colon cancer cells.

A colorectal adenocarcinoma cell line, HT29 (ATCC No. HTB-38) was used as the model for this study. During normal cell culture, HT29 cells remained in an undifferentiated state. Changing the chemical composition of the growth media used can induce differentiation, allowing researchers to compare proliferating cells to non-proliferating cells. Upon differentiation the HT29 cells form tight junctions, creating a monolayer of cells that also form a brush border membrane.

SECTION 1-7: Outline of the project

The aim of the present thesis is to analyze isoform specific (isoform B and myopodin) changes in expression upon differentiation, using a colon cancer cell line as a model. Isoform B and myopodin differ only at the N-terminal end. Knowing that Synpo2 is often classified as a tumor suppressor, the effects of over-expressing either isoform B or myopodin should negatively affect the rate of proliferation and cell migration.

The first objective of the study was to determine which of the Synpo2 isoforms are expressed in HT29 cells at an mRNA and protein level, in a differentiated and undifferentiated state. RT-PCR was performed to determine the expression of isoform A, B and C at an mRNA level in a differentiated and undifferentiated state. Due to the similarity between isoform B and myopodin, long-range PCR and Western blot analysis had to be performed to determine if there was a difference in expression between the two isoforms. Myopodin, not isoform B, was found to be expressed both at an mRNA and protein level. Similar in composition, but different in expression, these isoforms were the main focus for this thesis. To better understand the function of myopodin and isoform B in cells, the full-length genes were cloned and used for

overexpression analysis. In parallel to overexpression, knocking down the expression of Synpo2 using siRNAs will aid in understanding its role within the cells.

CHAPTER 2:

Synaptopodin-2 Isoform B and Myopodin Expression Paper

A NOVEL NUCLEOLAR LOCALIZATION OF A SYNAPTOPODIN-2 ISOFORM IN PROLIFERATING HT29 CELLS

Urankar, S.E.*, Schmidt, M.*, Baxley, T.A.[1], Chalovich, J.M.[1] & Scemama, JL*

*Department of Biology, East Carolina University, Greenville, NC 27858

[1]Department of Biochemistry & Molecular Biology, 5E-122 Brody Building, Brody School of Medicine at East Carolina University, 600 Moye Blvd., Greenville, NC 27834, USA

Email: scemamaj@ecu.edu

Fax: 252-328-4178

Phone: 252-328-6313

ABSTRACT

Synaptopodin-2 has been described as a hub protein that associates with cytoskeletal proteins, such as actin and other actin associating proteins. In bladder and prostate cancer (Lin et al., 2001; Sanchez-Carbayo et al., 2003; Jing et al., 2004; Yu et al., 2006; Cebrian et al., 2008; De Ganck et al., 2009), synaptopodin-2 has been suggested to act as a tumor suppressor gene and its loss of expression by deletion or hypermethylation leads to an increased rate of invasiveness. More recent studies have shown that the role of synaptopodin-2 is more complex and may be dependent on the diverse signals found in the tumor microenvironment (Kai et al., 2012). Studies on synaptopodin-2 function are also complicated and manifold due to the presence of multiple isoforms. At least 5 synaptopodin-2 isoforms have been described. Two of these isoforms, myopodin and isoform B possess the same full-length C-terminal exon. This project analyzes the localization and expression of both these isoforms in HT29 colon adenocarcinoma cells using immunofluorescence, RT-PCR, and Western blot analysis. Our results demonstrate that myopodin but not synaptopodin-2 isoform B is expressed in HT29 cells. We also identified a potentially new synaptopodin-2 isoform, which is predominantly expressed in the nucleoli of undifferentiated HT29 cells. Furthermore, this nucleolar expression is altered upon cell differentiation.

INTRODUCTION

Synaptopodin-2 is a member of the synaptopodin family and has been shown to bind to and promote actin polymerization (Leinweber et al., 1999; Beall & Chalovich, 2001); it also associates with several other cytoskeletal proteins (Asanuma et al., 2005; Pham & Chalovich, 2006; Yu & Luo, 2006; Shen et al., 2005). Synaptopodin-2 possesses 3 α-actinin binding sites and has been shown to colocalize with α-actinin and filamin during muscle development (Renegar et al., 2009; Linnemann et al., 2010). One α-actinin isoform, α-actinin-4, has been shown to shuttle from the cytoplasm to the nucleus depending on the cell cycle phase (Kumeta et al., 2010). Similarly, Synpo2 expression has been shown to translocate from the cytoplasm to the nucleus (Weins et al., 2001), suggesting a possible link between Synpo2 and α-actinin-4. The role that Synpo2 plays within the nucleus is unclear and previous studies present contradicting results. Some groups have suggested a tumor suppressor role for Synpo2 (De Gank et al., 2009; Lin et al., 2001; Cebrain, 2008), while others have demonstrated that Synpo2 may act as a tumor activator and increase invasiveness in prostate cancer cells and mouse myoblast cells (DeGanck et al., 2009; Van Impe et al., 2003).

Five isoforms of Synpo2 have been characterized as the product of alternative splicing (Chalovich & Schroeter, 2010). These isoforms mainly differ by their C terminus (isoform A, B and C) and myopodin is a truncated version of isoform B, which lacks the N-terminus and is encoded by exon 1, 2, 3, and part of 4a. The smallest of the synaptopodin-2 isoforms is composed of exons 1, 2 and only a small portion of exon 6. It is likely that these isoforms play different roles and/or are expressed in different compartments of the cell. Most of the studies in this introduction did not consider that different cell types may express different Synpo2 isoforms or that different isoforms may be expressed in different cellular compartments. To better understand the functions associated with Synpo2, it is necessary to analyze individual isoforms.

In this study, we analyzed the expression pattern of myopodin, a specific Synpo2 isoform, in HT29 cells. Using RT-PCR, Western blot analysis, and immunocytochemistry with an isoform specific antibody against the C-terminus (exon 4b), we showed the localization of this isoform to better understand some of its possible roles in cancer cells. We showed that in proliferating HT29 cells, myopodin is mainly expressed in the nuclei with the strongest expression being observed in the nucleoli. Western blot analysis shows the presence of a possible new isoform of approximately 55 kDa. Interestingly this new isoform is found mainly in the nucleolus of HT29 cells. The nucleolar expression in proliferating cells may suggest a role in transcription activity. Upon cell differentiation, when cells are no longer proliferating and transcriptional activity is only at a basal level, expression is translocated from the nucleoli to the cytoplasm.

MATERIALS AND METHODS

Cell culture. HT29 cells (ATCC: HTB-38) were grown in DMEM/F12 (Gibco-BRL Life Technologies, Grand Island, NY, USA), supplemented with 10% fetal bovine serum, 100 µg/mL streptomycin and 100 IU/mL penicillin and maintained at 37^{O}C in a humidified 5% CO_2 incubator. Differentiation was induced by supplementing normal media with 5mM sodium butyrate, as previously described (Augeron and Laboisse, 1984).

Antibodies. The NC_781 is a polyclonal antibody generated by immunization of a rabbit with a keyhole limpet hemocyanin-conjugated peptide. The antibody was affinity purified against the synaptopodin-2 4b exon peptide sequence: VWKPSVVEE.

Immunocytochemistry. HT29 cells were seeded on 18 mm^2 glass coverslips and allowed to adhere overnight under normal culturing conditions. Each of the following steps were carried out at room temperature. Cells were washed with 1X PBS and fixed in 3.7 % formaldehyde in 1X PBS for 8 minutes. Cells were washed in 1X PBS, permeated with 0.1 % Triton-X100 in 1X PBS

for 4 minutes, and blocked in 10 % FBS in 1X PBS for 45 minutes. The primary NC_781 antibody was diluted 1:600 with 10 % FBS in 1X PBS and incubated with the cells for 45 minutes. The cells were then washed in 1X PBS and the secondary antibody (Sigma F1262), diluted 1:150, was incubated with the cells for 45 minutes. The specificity of the antibody was verified by preabsorption with the corresponding exon 4b peptide sequence that had been used for immunization. Cell samples were visualized using an Olympus BX40 microscope, equipped with a QColor 5 Olympus camera and the Qcapture Pro 6.0 program and the Olympus Confocal Microscope.

Long-range PCR. Primers were designed to amplify full-length isoform B and myopodin genes, using the Expand Long Template PCR System (Roche). The forward primers designed for isoform B and myopodin were: 5'GAG AAGCTTAAAACATGGGCACAGGGGATTTTATCTGC 3' and 5'GAGAAGCTTAAAACATGTTTAAGAAGCGACGTCGGAGG 3', respectively. A common reverse primer was used: 5'GAGGGATCCTT AGTGATGGTGATGGTGATGGCCCCCTCCCTCTTCCACAACAGATGGTTTCC3'. The optimal annealing temperature determined for the primer sets was 60^{O}C.

Western blot. Cells were lysed in an ice-cold lysis buffer (20mM Tris-HCl pH 7.5, 137 mM NaCl, 2 mM EDTA pH 8, 1 % NP-40, 10 % Glycerol). The lysis buffer was supplemented with Pierce Protease Inhibitor Cocktail (Thermo Fisher Scientific, 88661) prior to use. Lysates were incubated for 30 minutes at 4^{O}C under constant agitation. Protein concentrations were determined through the Pierce assay using bovine serum albumin as a standard. Western blotting was performed as described (Towbin, 1979) with the NC_781 antibody. Proteins were visualized by Immobilon Western Chemiluminescent HRP Substrate (Millipore, WBKLS0100) and visualized using the Chemidoc XRS System.

Statistics. Three hundred random cells were analyzed and the number of instances when NC_781 expression was colocalized with nucleolin was determined. This percentage was compared to the number of times NC_781 was expressed and did not colocalize with nucleolin or when nucleolin was expressed without colocalizing with NC_781. Statistical significance was determined by a two-tailed t-test ($p < 0.05$).

RESULTS

RT-PCR analysis shows that myopodin not synaptopodin-2 isoform B is expressed in HT29 cells

In order to determine which spliced variants of Synpo2 mRNA were expressed in HT29 cells, we designed a set of primers to amplify target variants using long range RT-PCR. Two forward primers were designed to anneal to the start ORF of isoform B (Synpo2StartF) or of myopodin (MyopodinForward) and a reverse primer that anneals to the end of exon 4b (Figure 5A). Human skeletal muscle cDNA was used as a positive control to validate each primer set (Figure 5B; Lanes 2 and 4). While we were able to amplify the myopodin splice variants from HT29 cells cDNA, we were not able to amplify Synpo2 isoform B (Figure 5B; Lane 3). These data suggest that myopodin, but not isoform B, is expressed in HT29 cells. These data were confirmed by Western blot analysis using whole cell lysates. The polyclonal affinity purified antibody used, NC_781, was designed to recognize an epitope encoded by exon 4b and was therefore recognizing specifically either isoform B or myopodin. Western blot analysis showed the presence of a 75 kDa protein (Figure 5C), which corresponds to the size of myopodin and we did not observe any higher molecular weight proteins. This data supports that HT29 cells express myopodin, not isoform B.

Interestingly, we repeatedly observed the presence of an unexpected 55 kDa protein on the western blots. This protein is believed to be an uncharacterized synaptopodin-2 isoform that probably utilizes an alternative start site further downstream than the myopodin start site. Three

possible alternative start sites were determined after analyzing the amino acid sequence that would yield proteins of 64 kDa, 63 kDa, or 54 kDa.

Myopodin's localization through immunofluorescence

To determine the domain of expression of myopodin within HT29 cells, we performed immunohistochemistry with the same antibody used for the western blot analysis. The immunofluorescence was mainly localized in the nuclei of proliferating HT29 cells. The immunofluorescence was more intense in punctate spots within the nucleus. The pattern observed was reminiscent of nucleoli localization. To confirm the nucleolar localization, we performed double staining experiments in which the cells were also stained with DAPI (Figure 6A). DAPI is a DNA stain that does not stain the nucleoli which mainly contain RNA molecules. The double staining experiment showed that the intense spots recognized by the NC_781 corresponded to regions not stained by DAPI. These results suggested that myopodin was expressed in the nucleoli. We also showed that myopodin colocalizes with nucleolin, a nucleolar protein (Figure 6B).

After analyzing several images of myopodin with nucleolin and DAPI, it became apparent that myopodin expression was not exclusively limited to nucleolar regions. A small percentage of instances analyzed showed that occasionally (11%) myopodin expression in the nucleus was not exclusive to the areas not stained with DAPI (Figure 6A arrowheads and C) or with nucleolar expression (data not shown). Also, in a smaller percentage of instances (6%), a nucleolar region was expressed without corresponding to myopodin expression (Figure 6A thick arrows and C). However, a majority of myopodin's expression (83%) was localized with the nucleolus of HT29 cells.

Figure 5: Expression pattern of Synpo2 in whole cell extracts from HT29 cells through RT-PCR and Western blot analysis

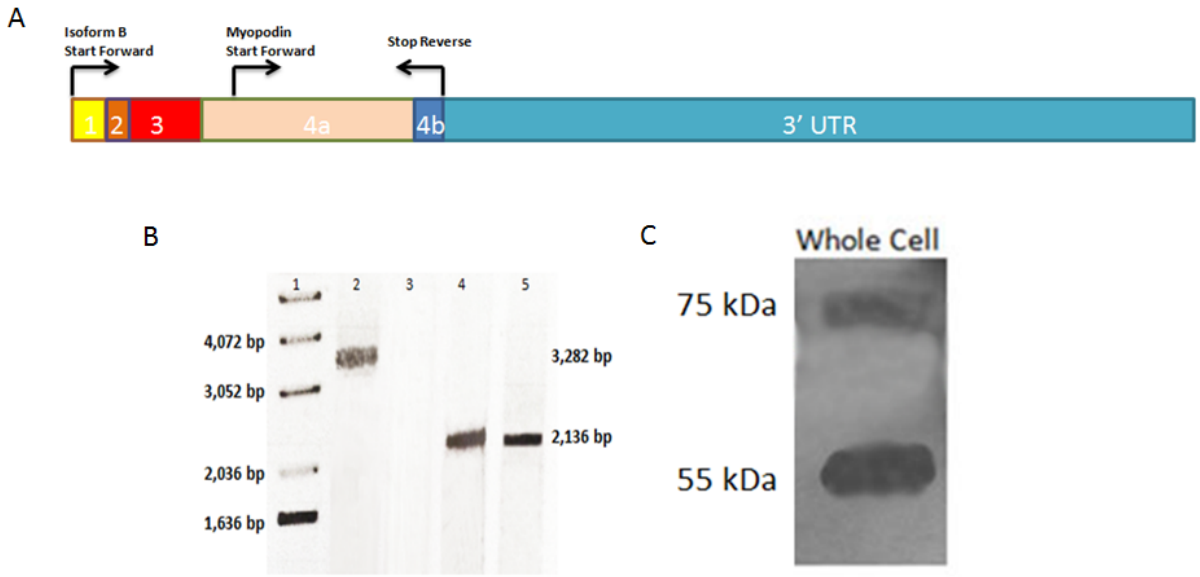

Figure 5: Expression of Synaptopodin-2 in HT29 cells. (A) A schematic representation of where the primers are designed to amplify the full-length open reading frame of isoform B and myopodin anneal. (B) RT-PCR results using primers described in A to amplify isoform B (lanes 2 and 3) and myopodin (lanes 4 and 5). Lanes 2 and 4 were positive controls for isoform B and myopodin, respectively, using human skeletal muscle cDNA. Lanes 3 and 5 were run from HT29 cDNA for isoform B and myopodin, respectively. (C) Western blot analysis on HT29 whole cell extract.

Figure 6: Immunofluorescence using a Synpo2 isoform specific antibody in undifferentiated HT29 cells

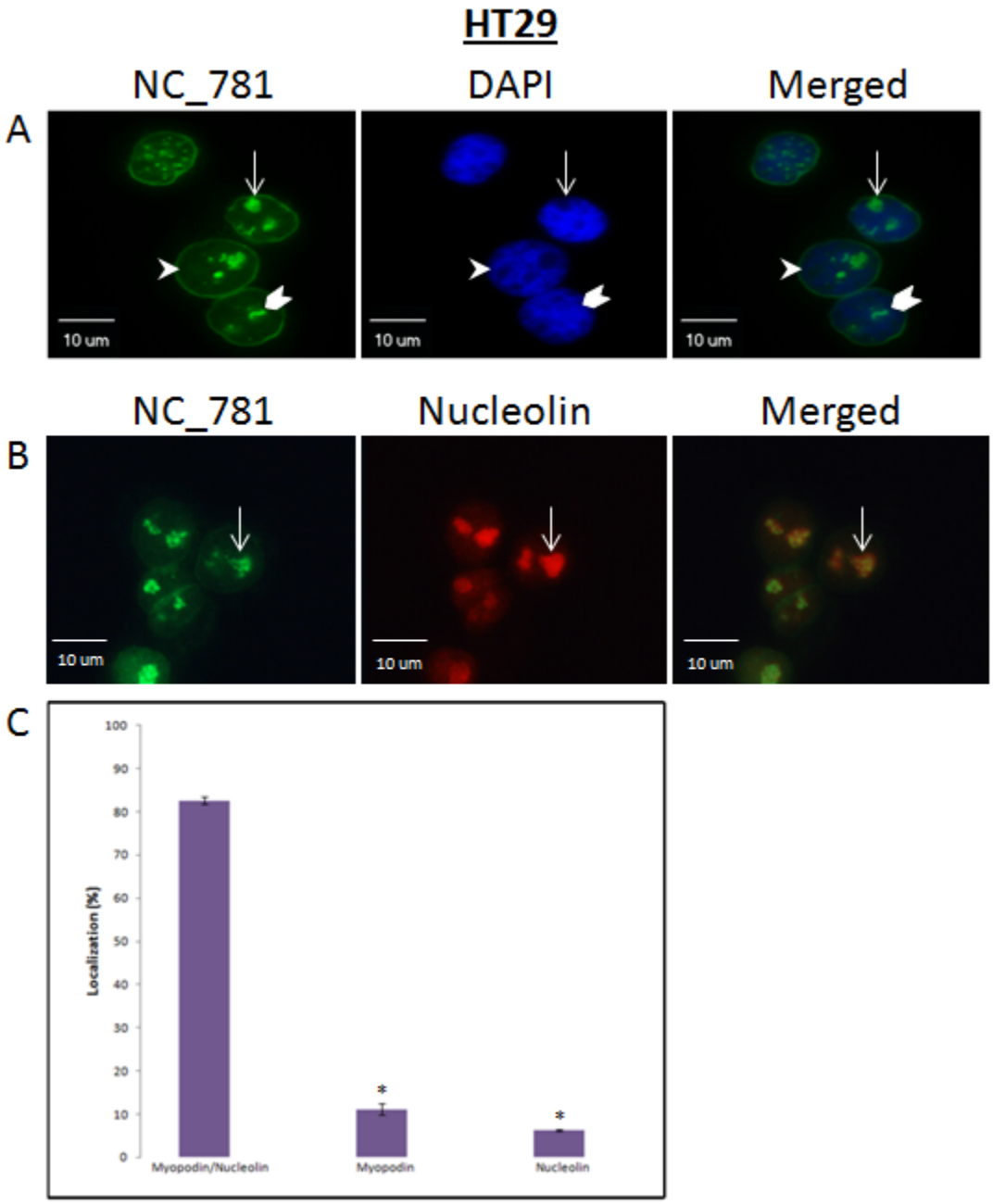

Figure 6: Immunofluorescence of myopodin in HT29 cells. (A) The NC_781 antibody recognizes an epitope specific for myopodin and was double stained with DAPI to show nuclear localization. (B) Myopodin colocalizes with nucleolin. Arrows highlight colocalization of myopodin with nucleolin; arrowheads highlight dark regions in DAPI stain that do not correspond to myopodin expression; thick arrows highlight myopodin expression that does not correspond to dark regions of DAPI stain. (C) Statistical analysis of myopodin and nucleolin expression pattern compared to its colocalization. Statistical significance was determined by a two-tailed t-test and denoted by * ($p < 0.05$).

Verification of nucleolar localization

In order to confirm the expression of myopodin obtained with the NC_781 antibody was truly nucleolar and not expressed on the nuclear membrane, a 3-dimensional image was taken of the HT29 cells using NC_781 and DAPI (data not shown). Another way we confirmed myopodin's nucleolar expression was to analyze its change in expression upon transcriptional inhibition. Nucleolar proteins will change in expression, by either increasing, decreasing, or translocating throughout the cell when transcription is inhibited. To inhibit transcriptional activity, HT29 cells were treated with actinomycin D and the expression of myopodin was analyzed at 2, 4, and 8 hours after treatment (Figure 7). Myopodin's expression went from being predominantly nucleolar to diffuse nuclear 2 hours post transcriptional inhibition (Figure 7A). The expression of myopodin remained nuclear at 4 and 8 hours after treatment (Figure 7B & C). This change in expression further verifies that myopodin is a nucleolar protein.

Myopodin expression through Western blot analysis

After analyzing the expression pattern of myopodin through immunofluorescence, Western blot analysis was performed on nuclear and cytoplasmic extracts from the HT29 cells to confirm nuclear expression of myopodin. Surprisingly, myopodin was expressed predominantly in the cytoplasmic extract, which was never seen through immunofluorescence. However, an undescribed 55 kDa Synpo2 variant was expressed exclusively in the nuclear extract (Figure 8). These data suggest a possible sixth undescribed synaptopodin-2 isoform that the NC_781 antibody recognizes through immunofluorescence predominantly in the nucleolus, that is not isoform B or myopodin.

Figure 7: Transcriptional inhibition through Actinomycin D treatment disrupts nucleolar localization of specific Synpo2 isoforms

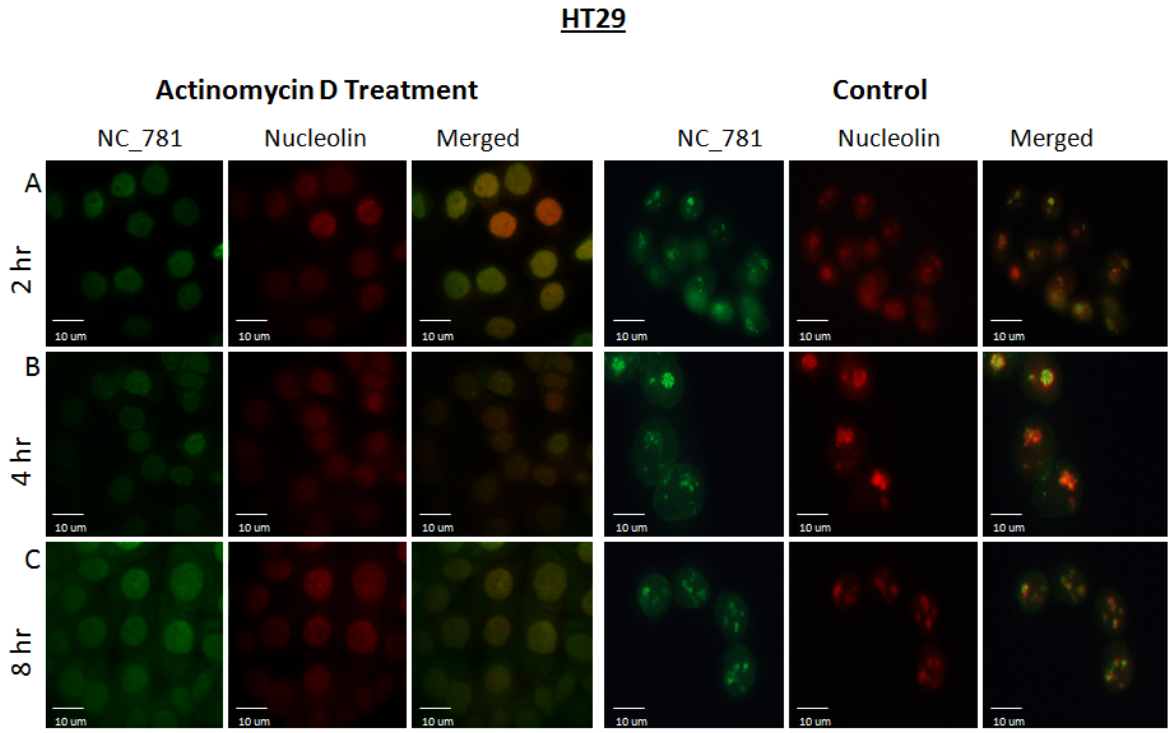

Figure 7: Nucleolar localization disrupted through transcriptional inhibition (A) Two hours post actinomycin D treatment; (B) four hours post actinomycin D treatment; (C) eight hours post actinomycin D treatment. HT29 cells were imaged through immunofluorescence using the NC_781 antibody for myopodin and nucleolin.

Immunofluorescence using a non-isoform specific antibody

A non-isoform specific antibody of synaptopodin-2 (pan antibody) was used to compare its expression pattern to that of the NC_781 isoform specific antibody. The pan antibody was capable of recognizing all known synaptopodin-2 isoforms, except for the smallest unnamed isoform that lacks exon 4a. The expression pattern of NC_781 (Figure 9A) was distinctly different from that of the non-isoform specific expression pattern of synaptopodin-2 (Figure 9B). The expression of NC_781 was exclusively located within the nucleus, with intensely stained and well-defined punctate spots in every cell (Figure 9A), whereas the expression pattern with the pan antibody was notably absent from the nucleus and almost solely expressed in the cytoplasm (Figure 9B).

One possible explanation for the difference in expression patterns is that the smaller, approximately 55 kDa protein seen through Western blot, lacks the epitope for the pan antibody. There are three possible alternative start sites that were identified through sequence analysis that would yield proteins of approximately 64 kDa, 63 kDa, and 54 kDa (Figure 9C). The start site that would produce a 54 kDa protein only contains a small portion of the pan antibody epitope. However, the start sites that would produce either a 64 kDa or a 63 kDa protein would also possess the pan antibody epitope (Figure 9C). When using the pan antibody for Western blot analysis, similar 75 kDa and approximately 55 kDa banding patterns are obtained (data not shown). This suggests that the unknown 55 kDa protein possess both the NC_781 and the pan antibody epitope; however, no known synaptopodin-2 isoform would be able to account for the differences in expression pattern through immunofluorescence, yet show similar expression through Western blot analysis.

Figure 8: Western blot of nuclear and cytoplasmic fractions from HT29 cells using isoform specific antibody

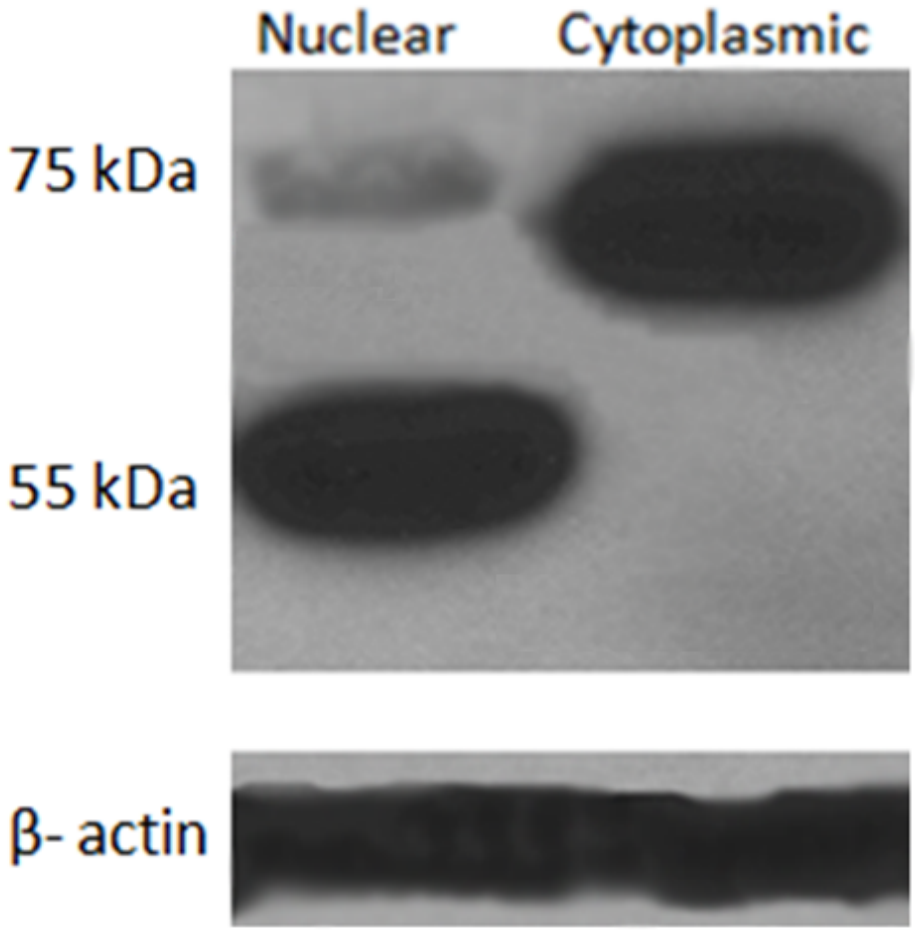

Figure 8: Western blot analysis of HT29 nuclear and cytoplasmic fractions. Comparing nuclear and cytoplasmic extracts from HT29 cells, using the NC_781 antibody shows a robust cytoplasmic band for myopodin. The unknown 55 kDa protein was exclusively localized to the nuclear extract.

Change in expression upon differentiation

In order to determine the change of expression upon cell differentiation, immunocytochemistry was performed on HT29 cells that had been exposed to differentiation media (5 mM sodium butyrate) for 3, 5, and 7 days. Upon cell differentiation, the NC_781 expression pattern went from being entirely nuclear, and predominantly nucleolar (Figure 6A), to a diffuse nuclear by days 3-5 (Figure 10A), and ultimately expressing exclusively in the cytoplasm by day 7 (Figure 10C). This change in expression suggested a translocation from the nucleoli of undifferentiated cells to the cytoplasm upon differentiation, using the NC_781 antibody. Interestingly, the NC_781 expression banding pattern did not change upon differentiation in Western blot analysis (Figure 10D). The only change detected through Western blot analysis was a decrease in intensity of bands upon differentiation compared to undifferentiated cells. When considering the change in expression pattern through immunofluorescence, but the lack of change through Western blot, this data suggests that synaptopodin-2 isoforms are not what is shuttling between cell compartments; but rather epitopes are either becoming exposed to allow antibody binding or are being masked through conformational changes to the protein or through a change in protein-protein interactions.

Figure 9: Expression of NC_781 isoform specific antibody compared to Synpo2 pan antibody expression pattern in HT29 cells

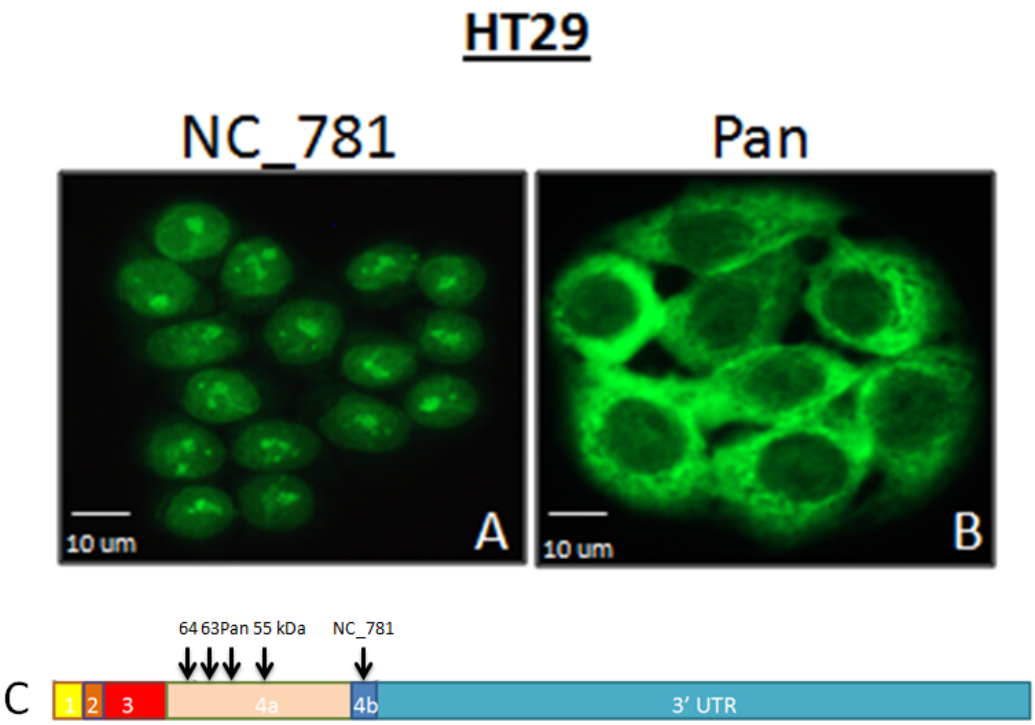

Figure 9: Expression of isoform specific antibody compared to non-isoform specific expression pattern. (A) The NC_781 antibody is specific for an epitope encoded by the 4b exon of myopodin (highlighted by the schematic in C). (B) The Pan antibody is non-isoform specific, recognizing an epitope on exon 4a, which is common to 4 of the 5 known synaptopodin-2 isoforms. (C) A schematic representation of where epitopes are located on the gene, as well as possible alternative start sites that would result in a new synaptopodin-2 isoform.

Figure 10: Change in Synpo2 expression pattern upon differentiation of HT29 cells

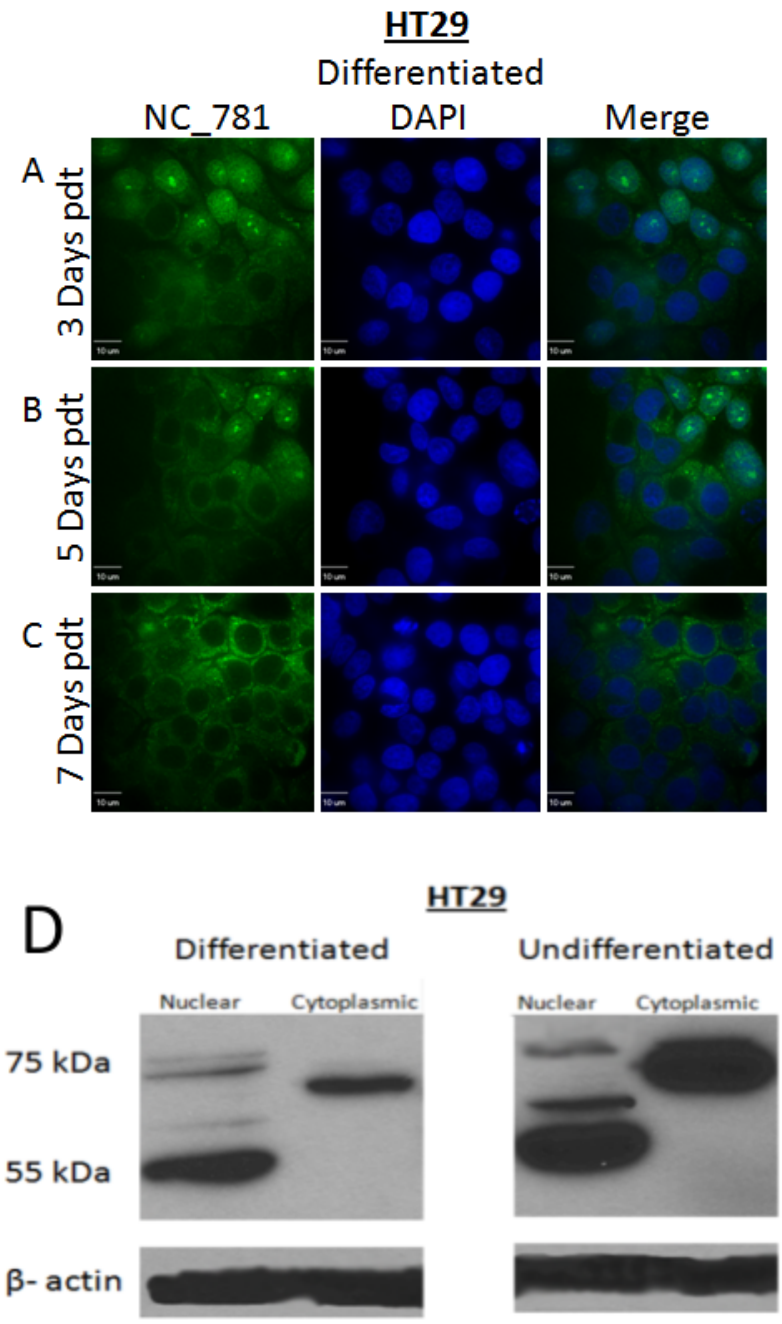

Figure 10: Change in Synpo2 expression pattern upon differentiation of HT29 cells. (A) 3 Days pdt shows an initial change in the expression pattern of NC_781 from nucleolar to a diffuse nuclear and even cytoplasmic. After 5 days of treatment (B) nucleolar expression is even more dispersed and by a full week of treatment, (C) expression pattern is solely localized to the cytoplasm. Pdt = post differentiation treatment. (D) Western blot analysis using the NC_781 antibody to compare expression of differentiated and undifferentiated HT29 cells.

DISCUSSION

It has been suggested that synaptopodin-2 has several possible roles within the cell (Asanuma et al., 2005; Beall & Chalovich, 2001; Yu & Luo, 2006; Schroeter & Chalovich, 2004; Kołakowski et al., 2004; Kai et al., 2012). Research groups have categorized synaptopodin-2 as a tumor suppressor because of its decreased expression in urothelial cancer (Sanchez-Carbayo et al., 2003) or its inactivation of expression in prostate cancer (Yu et al., 2006). Other groups have suggested a contradicting role for synaptopodin-2 as a tumor activator, because over expression of synaptopodin-2 in normally non-invasive human endothelial kidney or mouse myoblast cells increased the cells invasiveness into a collagen matrix (Van Impe et al., 2003; De Ganck et al., 2009). Realizing that synaptopodin-2 isoforms respond differently to chemokinetic stimuli (Kai et al., 2012) implies the possibility of their functionally discrete roles within the cell. This study focused on the expression profile of synaptopodin-2 isoform B and myopodin, to better understand their effects within a colorectal cancer cell line. Synaptopodin-2 isoform B and myopodin are the only two synaptopodin-2 isoforms that possess the same full-length C-terminal exon 4B; however, myopodin is truncated at the amino terminus and is completely missing exon 1-3, as well as a portion of exon 4A. For the purpose of this study, synaptopodin-2 isoform B and myopodin were analyzed in colon cancer HT29 cells.

Our goal was to study the expression of isoform B and myopodin at an mRNA and protein level within the cell using PCR, Western blot and immunofluorescence with the antibody NC_781 that was specific for exon 4B. Other groups have suggested that synaptopodin-2 resides in the nucleus (Weins et al., 2001; Faul et al., 2007; Cebrian et al., 2008; Pompas-Veganzones et al., 2016). Interestingly, our lab has previously shown that Synpo2 isoforms A and D are exclusively expressed in the cytoplasm of HT29 (Shortt, unpublished data). In this study we saw no expression for isoform B in undifferentiated or differentiated

HT29 cells. However, myopodin, the smallest named Synpo2 isoform, was expressed in HT29 cells at an mRNA and protein level in the nucleus of undifferentiated and differentiated cells. Unexpectedly, we detected an unknown protein of approximately 55 kDa, in addition to myopodin at 75 kDa, through Western blot analysis using an exon 4B specific antibody, NC_781. The NC_781 antibody was raised against the 9 amino acid peptide of exon 4B and affinity purified. Despite the specificity of the NC_781 antibody for Synpo2 exon 4B, cross-reactivity of the antibody needs to be considered. There are several 55 kDa nucleolar proteins whose sequences were examined for potential cross-reactivity with the NC_781 antibody. However, BLAST analysis showed no other protein with a similar sequence that would be able to act as an epitope for this antibody. These results suggest the 55 kDa protein is another Synpo2 isoform. For the purpose of this discussion, we will refer to this possible Synpo2 isoform as variant X.

Initial immunofluorescence data gathered from undifferentiated HT29 cells revealed all expression detected by the NC_781 antibody was exclusively nuclear, and even more interestingly, it was predominantly nucleolar. To our knowledge this is the first report of nucleolar localization of any synaptopodin-2 isoform, which suggests possible transcriptional regulation activity within the cell. As a way to confirm nucleolar expression detected with the NC_781 antibody, we were able to show colocalization of nucleolin (a well-documented nucleolar expressed protein) with the nucleolar expression detected by the NC_781 antibody. Additionally, we inhibited transcriptional activity of HT29 cells by treating them with actinomycin D for 2, 4, and 8 hours. The nucleolar localization exhibited in untreated cells was lost and a more diffuse nuclear distribution was detected. These results verified the protein recognized by NC_781 through immunofluorescence as a nucleolar protein.

When nuclear and cytoplasmic extracts were made from undifferentiated HT29 cells, we expected to see a band corresponding to the size of myopodin intensely expressed in the nuclear extract and no expression in the cytoplasmic extract. These results would support the data collected through immunofluorescence. Surprisingly, an extremely robust 75 kDa band,

which corresponds to myopodin, was seen in the cytoplasmic extract and only a faint band was detected in the nuclear compartment. Another unexpected piece of data that was provided through the Western blot was the detection of a smaller, undescribed 55 kDa (variant X) protein that was exclusively and intensely expressed in the nuclear extract. Western blot using nucleolar extracts made from HT29 cells (data not shown) showed an extremely robust band at approximately 55 kDa and nothing that would correspond to myopodin. These data suggest that it is the undescribed variant X that is actually localizing within the nucleolus, not myopodin.

Similar to the results reported by Weins et al. in mouse myoblast cells (2001), our immunofluorescence data shows myopodin is localized in the nucleus of undifferentiated cells but is predominantly expressed in the cytoplasm upon differentiation. These findings would support myopodin's role as a tumor suppressor, which is supported by previously unpublished data we collected that showed the overexpression of myopodin in Hela cells resulted in reduced proliferation rates (Harkins, unpublished data). Our immunofluorescence images support a change in expression pattern from undifferentiated to differentiated HT29 cells. This change in myopodin expression upon differentiation may affect cell cycle activity through its association with the actin cytoskeleton. The possible undescribed Synpo2 isoform, variant X, which was shown to be expressed largely in the nucleolus of undifferentiated HT29 cells through immunofluorescence, was dramatically reduced upon cell differentiation, in agreement with our Western blot data. Interestingly, this 55 kDa protein was never detected in cytoplasmic extracts analyzed through Western blot, regardless of the cell's state of differentiation. The only notable changes from undifferentiated nuclear and cytoplasmic protein extracts to differentiated nuclear and cytoplasmic protein extracts were from variability in band intensities, as there was no change in the banding pattern detected through Western blot. This suggests the cytoplasmic expression observed by immunofluorescence upon differentiation is solely attributed to changes in myopodin through transcription/translation and not translocation.

It is remarkable that cytoplasmic extracts yield a more robust band through Western blot in undifferentiated HT29 cells compared to expression of differentiated cells, because our

immunofluorescence data (which used the same antibody) detected virtually no cytoplasmic expression in undifferentiated HT29 cells. One possible explanation for this discrepancy could be attributed to the hub protein properties associated with synaptopodin family members. It is reasonable to consider that myopodin expression in the cytoplasm is not detected through immunofluorescence because the NC_781 antibody epitope is blocked by any one of myopodin's several known binding partners. However, the denaturation process involved with Western blot analysis would dissociate myopodin from its binding partners, allowing the antibody access to the epitope.

Recent studies have suggested the importance of maintaining the appropriate ratio of cytoplasmic Synpo2 to nuclear Synpo2 for proper cell function (Gao et al., 2020). Loss of nuclear Synpo2 expression has been associated with poor clinical outcomes in bladder cancer (Carbayo-Sanchez et al., 2003). Additionally, increased cytoplasmic expression to nuclear expression of Synpo2 has been correlated to a significantly higher reassurance rate of liver cancer (Gao et al., 2020). However, this data was collected using a non-isoform specific region of the Synpo2 genome. To our knowledge, this study is the first to suggest that changes in cytoplasmic and nuclear expression of Synpo2 is not solely attributed to nuclear-cytoplasmic translocation, but instead to changing compartmental levels of isoform expression. Our laboratory has previously reported that the role Synpo2 plays, as either a tumor suppressor or activator, is isoform dependent (Shortt, unpublished data). Understanding the changes in expression of individual Synpo2 isoforms is critical to better understand the overall function it has within the cell.

Using the NC_781 antibody, designed exclusively to detect Synpo2 isoform B and myopodin expression, we detected nucleolar expression of a possible uncharacterized Synpo2 isoform at 55 kDa. To our knowledge, our lab is the first to detect nucleolar expression of this synaptopodin-like protein. The nucleolar synaptopodin-like expression we saw in undifferentiated HT29 cells suggests a highly critical role for normal cell function. Nucleoli are prominent substructures located within the nuclei of cells and are connected to cell growth,

division, and proliferation. The nucleoli have been predominantly associated with the biogenesis of rRNA by RNA polymerase I and the assembly of ribosomal subunits (Busch & Smetana, 1970; Hadjiolov, 1985). It is estimated that rRNA synthesis accounts for approximately 50% of the total RNA production in an actively growing and dividing cell (Zylber & Penman, 1971). If expression of Synpo2 has an effect on rRNA synthesis, then by association it would affect the cells ability to proliferate. In addition to its ribosomal production role of the nucleoli, it has become evident; the nucleolus is not limited to these functions. Over 700 proteins have been characterized within or in association with these structures and still a significantly large number of uncharacterized/novel proteins that are yet to be described for their role within the nucleolus (Boisvert et al., 2007). Our findings suggest the novel nucleolar expression of the previously uncharacterized Synpo2 isoform may be critical for normal cell function.

In agreement with our labs previous findings, it seems the effects of Synaptopodin-2 as either a tumor suppressor or activator are isoform dependent, as the expression of individual isoforms are altered through differentiation. These findings, along with the nucleolar localization of Variant X, suggest a more complex role for Synaptopodin-2 in cell cycle progression than what was previously described.

CHAPTER 3: MATERIALS AND METHODS

Cell Culture

HT29 cells were obtained from ATCC (Cat number: HTB38) and were used as the model for this research project. For normal cell culture, the HT29 cell line was cultured in DMEM/F12 (Invitrogen), supplemented with 10% fetal bovine serum (FBS), penicillin and streptomycin (100U and 100 µg/ml, respectively). Normal cell conditions were 37°C in a humidified CO_2 incubator (5 % CO_2).

HT29 Differentiation

HT29 cells were differentiated using sodium butyrate, following a previously described protocol (Augerson and Laboisse, 1984). Cells were seeded on coverslips that were placed in 35mm Petri dishes. For each Petri dish, 750,000 cells were plated and allowed to adhere and proliferate in normal DMEM/F12 for 48 hours. The normal media was aspirated then replaced with normal DMEM/F12 media supplemented with sodium butyrate at a 5 mM final concentration. The cells were maintained in sodium butyrate supplemented media that was changed daily for 7 days.

RNA Extraction

RNA was extracted from cells in culture using the following procedure and reagents from the RNeasy kit (Qiagen). Cells were grown in T75cm^2 flasks until 90% confluent. Once cells reached approximately 5 million total cells, the media was removed and cells were washed with 5 mL with 1X phosphate buffered saline (PBS). After removing the 1X PBS, cells were detached

using 0.05% trypsin in EDTA (Gibco). Once the cells had detached, 5 ml of complete DMEM/F12 media was added to the flask. The cells were transferred into an RNase-free microcentrifuge tube and were pelleted at 300 x *g* for 5 minutes. The supernatant was completely aspirated and 600 µl of Buffer RLT was added and mixed thoroughly to resuspend the pellet. The cell lysate was then homogenized by passing the solution through a 20-gauge needle 5 times. One volume of 70% ethanol was added to the homogenized lysate and mixes well through pipetting. The homogenized lysate was then transferred to an RNeasy spin column, placed in a 2 ml collection tube, and was centrifuged at 1,000 x *g* for 15 seconds. The flow-through was discarded. Next, 700 µl of Buffer RW1 was added to the spin column and centrifuged again at 1,000 x *g* for 15 seconds. The flow-through was again discarded. To the spin column, 500 µl of Buffer RPE was added and centrifuged again for 15 seconds at 1,000 x *g*. An additional Buffer RPE wash was performed except that the column was spun for 2 minutes at 1,000 x *g*. A dry spin was then performed for 1 minute at 1,000 x *g* to ensure all the ethanol from the wash solution was removed from the spin column membrane. The spin column was then placed in a new 1.5 ml collection tube and 50 µl of RNase-free water was added directly to the membrane of the column and allowed to incubate at room temperature for 1 minute. The RNA was then eluted from the spin columns membrane by centrifuging for 1 minute at full speed. The total RNA extracted was quantified using the NanoDrop 2000 (Thermo Scientific) and stored at -80°C.

cDNA Synthesis

Total RNA was used to synthesize cDNA, after first undergoing a DNase treatment to remove any genomic DNA contamination (Turbo DNase Kit, Ambion). In brief, to a 5 µg solution of RNA sample, 0.1 volume of 10X TURBO DNase buffer and 0.5 µl TURBO DNase (2 U/µl) was added, and mixed gently. The samples were incubated at 37°C for 30 minutes then an

additional 0.5 µl of TURBO DNase was added and the samples were incubated at 37°C for an additional 30 minutes before adding 0.1 volume of DNase Inactivation Reagent. Samples were incubated at room temperature for 5 minutes, mixing periodically, before being centrifuged at 10,000 x *g* for 1.5 minutes and the supernatant was transferred into a new test tube. Five µg total purified RNA was aliquoted into 0.5 ml test tubes. One µl of 50 µM Oligo$(dT)_{20}$ primer or 1 µl of the 30µM gene specific RT primer (5' GCTAGGCATTCTCAGGGACTCAAG 3') and 1 µl of 10 mM dNTP were mixed will then added. The final volume was adjusted to 10 µl with sterile water. Samples incubated at 65°C for 5 minutes and then were transferred to ice for 1 minute. To each RNA/primer mix sample, 2 µl of 10X RT buffer, 4 µl of 25 mM $MgCl_2$, 2 µl of 0.1 M 0.1 DTT, 1 µl of RNase out (40 U/µl), and 1 µl of Superscript III RT (200 U/µl) were added. The samples were then incubated for 50 minutes at 50°C, and then at 85°C for 5 minutes. Finally 1 µL of RNase H was added and incubated for 20 minutes at 37°C. The resulting cDNA was cleaned, quantified with the NanoDrop and stored at -20°C.

Reverse Transcription Polymerase Chain Reaction (RT-PCR)

The cDNA synthesized from HT29 total RNA is used as the template for PCR. A PCR core mix is prepared by combining 15.125 µl of sterile water, 2.5 µl of 10X PCR buffer, 0.75 µl of 50 mM $MgCl_2$, 0.5 µl of 10 mM dNTPs, and 0.125 µl of Taq polymerase per reaction, in a test tube. The PCR core mix was then added to individual 0.2 ml PCR tubes that contained 1 µl of cDNA template and 2.5 µl of a 30 nM forward and 2.5 µl of a 30 nM reverse primer. A negative control tube was prepared in which the cDNA template was omitted and 1 µl of distilled autoclaved water added. These samples were placed in a thermocycler. The optimal annealing temperatures for each primer set was determined by running a temperature gradient ranging from 55-65°C. The thermocycler was programmed to denature the cDNA at 94°C for 2 minutes, then perform 40 cycles as follows: 94°C for 1 minute, the specified annealing temperature for

the primer set (Table 2) for 45 seconds, and 74°C for 1.5 minutes for elongation. The forward primers, for the individual variants, were designed to anneal to a sequence in the common 4a exon (Figure 1). Each reverse primer was designed to anneal to a sequence for their unique exon or in the 3' UTR. PCR products were analyzed on an agarose gel. 1X TAE buffer (Table 3) was used. Agarose gels were run for 1.5 hour at 90 volts.

Cloning

To analyze gain of function of synaptopodin-2 in HT29 cells, primers were designed to amplify the full length gene of isoform B and the closely related myopodin (see primer sequences in Appendix). The forward primer was designed to have a polymerase recognition clamp site, a HindIII restriction enzyme sequence, a Kozak sequence, followed by the start codon with the first 21 nucleotides of the coding gene sequence. The reverse primers were designed to anneal to the last 23 nucleotides in exon 4b on the 3' end of the gene, followed by a 3 glycine spacer, a 6XHIS-tag, a stop codon, and a BamHI restriction enzyme cleavage site.

The full length coding sequence was amplified through long range PCR, double digested with HindII and BamHI restriction enzymes, and ligated into the pcDNA4/TO vector (Figure 5). After ligation, the clone was amplified using E. *coli* and was selected for using ampicillin. The cloned sequences were confirmed for accuracy through sequencing. The transformed plasmid was then used to transfect HT29 cells.

Figure 11: pcDNA4/TO expression and pcDNA6/TR regulatory vectors

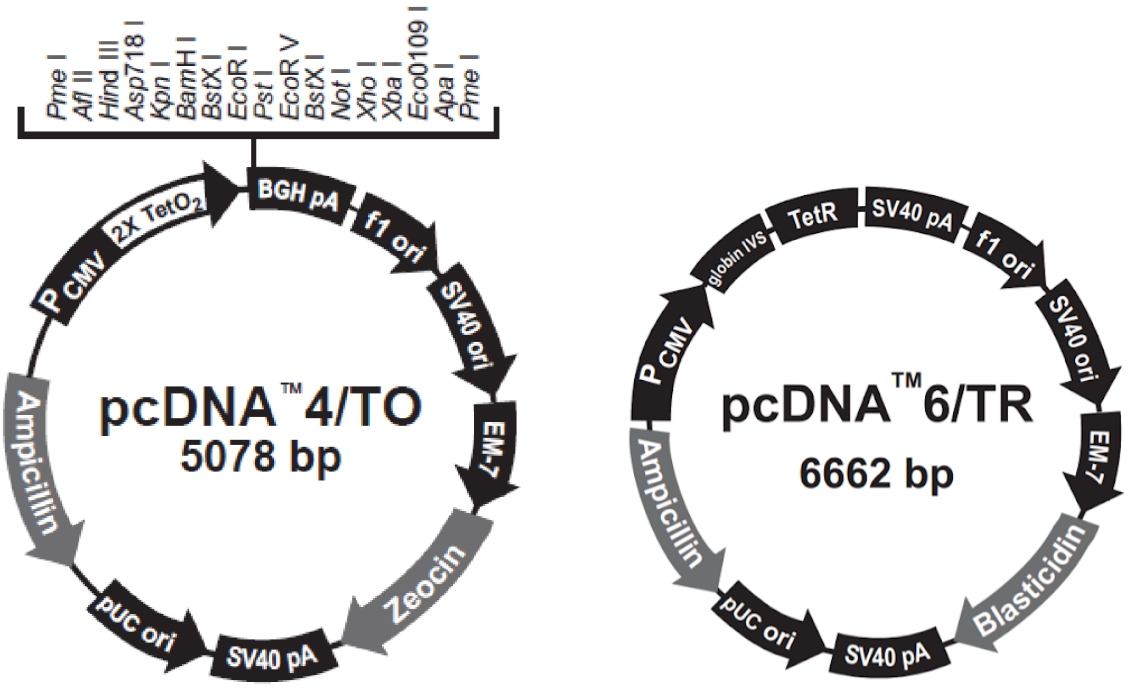

Figure 11: T-REx pcDNA4/TO mammalian expression vector and the pcDNA6/TR regulatory vector, purchased from Invitrogen. BamHI and HindIII restriction enzyme sites were used to insert the amplified PCR products into the pcDNA4/TP expression vector.

Transfection into HT29 Cells

HT29 cells were transfected using Lipofectamine 2000 (Invitrogen). Briefly, 0.5-2 10^5 cells were plated in 500 µl of 10% FBS supplemented DMEM/F12 without antibiotics in 24 well plates 24 hours before the transfection. The plasmid DNA was diluted in Opti-MEM I medium, following the manufacturer's recommendation (Invitrogen). The cells were cotransfected with the pcDNA6/TR (Figure 5) (Invitrogen) at a ratio of 6:1 (w:w) pcDNA6/TR:pcDNA4/TO plasmid with DNA insert. The pcDNA6/TR plasmid expresses the Tet repressors that repressed expression of the gene of interest inserted in the pcDNA4/TO plasmid. Lipofectamine 2000 transfection reagent was diluted in Opti–MEM I medium. After incubating at room temperature for 5 min, the diluted DNA was combined with the diluted Lipofectamine 2000 in a total volume of 100 µl/well to achieve a 1:3 ratio (DNA (µg) to lipofectamine (µl)). After 20 minutes at room temperature the 100 µl of diluted DNA and Lipofectamine 2000 was added to each well containing cells and medium. Cells were incubated at 37°C in a CO_2 incubator for 18-48 hours (medium was changed after 4-6 hours). The cells were passaged at a 1:10 ratio into fresh growth medium 24 to 48 hours after transfection, and selected with Zeocin and Blasticidin 24 hours later.

Cell Selection through Antibiotic Screening

Cell selection was performed using Zeocin, which upon activation will bind and cleave DNA, leading to cell death in untransfected HT29 cells. The cells that are Zeocin-resistant will continue to grow and divide normally. In order for accurate cell selection, the minimum concentration of Zeocin required to kill the HT29 cell line was first determined to be 800 µg/ml. This was determined using a testable range of concentrations for Zeocin, which in mammalian cells is 50-1000 µg/ml. Briefly, 8,000 cells/well were seeded in a 96 well-plate in normal media for 24 hours. The normal media was removed and media with varying concentrations (0, 50,

100, 200, 400, 600, 800, and 1000 µg/ml) of Zeocin was added. This selective media was changed every 3-4 days for 14 days. The appropriate working concentration of Zeocin in the selective media was the amount that killed the majority of the cells within 2 weeks. Cells that are sensitive to Zeocin will undergo morphological changes (increasing in cell size, altering the cell shape, the appearance of empty vesicles), which eventually lead to a complete breakdown of the cell. The selective media concentrations were performed in triplicate. Cell viability was determined through MTT assays (described below).

A double antibiotic selection process had to be used, since cells were cotransfected with plasmids that differed in antibiotic resistance. The pCDNA4/TO vector was screened for using Zeocin, whereas the pCDNA6/TR vector had to be screened for using Blasticidin. The minimum concentration of Blasticidin was determined to be 7.5 µg/ml, following the selective procedure listed for Zeocin, differing only in the antibiotic concentrations used (0, 1, 2.5, 5, 7.5, 10, 12.5, and 15 µg/ml). Having a dual selection process ensured that only the cells that survived possessed both plasmids necessary to express genes of interest.

Generating Stable HT29 Cell Lines

To generate stable HT29 cell lines that were able to inducibly express the gene of interest, the cells were first transfected and plated into 100mm culture plates. Once transfected, the cells were washed with 1X PBS and fresh complete DMEM/F12 media was then added to the cells. Between 48-72 hours after transfection the cells were split at varying densities into fresh media containing the selective Zeocin and Blasticidin antibiotic concentrations. The cells were maintained in the selective medium, replenishing every 3-4 days, until the cell foci were identified. The colonies that were picked as viable were transferred to 48-well plates then allowed to grow to near confluency before transferring them into a larger plate. The HT29 cells

were maintained in media containing 800 µg/ml of Zeocin and 7.5 µg/ml Blasticidin, to prevent the growth of sensitive cells.

MTT Assay to Analyze Cell Viability

In addition to the growth curve to analyze cell growth, a 3-*(4,5-Dimethylthiazol-2-Yl)*-2,5-Diphenyltetrazolium Bromide (MTT) assay can be performed to assess the proliferation and viability of the cells. This is done by seeding 500 cells/100 µl in complete DMEM/F12 per well, in a 96 well plate and incubating for 24 hours. After incubating, the media is removed and replaced with 100 µl of fresh, complete DMEM/F12 and 10 µl of 12mM MTT (Ambion). The wells are not mixed. Control wells are also made to contain 100 µl of complete DMEM/F12 media and 10 µl of MTT. The plate is incubated at 37^{o}C with 5% CO_2, for 4 hours. Samples are mixed with a pipette, avoiding the formation of bubbles. The plate is measured at 540nm.

Over Expression

The pcDNA4/TO expression vector contains two tetracycline operator 2 ($TetO_2$) sites within the cytomegalovirus (CMV) promoter, which allows for tetracycline-regulated gene expression through cotransfected with the pcDNA6/TR vector. Tet repressor molecules, which are expressed from the pcDNA6/TR plasmid, bind the $TetO_2$ sequence to prevent transcription of the desired genes. The addition of tetracycline to the cells will reduce the repression of the hybrid CMV/$TetO_2$ promoter in the pcDNA4/TO vector, which will allow the cells to express the Synpo2 genes of interest. Depending on the efficiency of the transfection, a 0.1-1 µg/ml final concentration of tetracycline is used to obtain optimal expression of the HT29 cell line.

Whole Cell Protein Extraction

Whole cell protein extracts, from HT29 cells, enabled further studies through western blot analysis to determine the expression of synaptopodin-2 isoform B and/or myopodin at a protein level. Whole cell lysate was made from HT29 cells. Sterile 1X PBS, the Nonidet-P40 (NP-40) buffer (20 mM Tris-HCl - pH 7.5, 137mM NaCl, 2mM EDTA - pH 8, 1% NP-40, 10% Glycerol), a rubber policeman, and microcentrifuge tubes were placed on ice 20 minutes prior to extraction to chill.

The cells were cultured to 75% confluency in a T75cm^2 flask before being harvested. To harvest the cells, the media was aspirated and 500ml of chilled 1X PBS was added directly to the cells then quickly removed. A protease inhibitor was added to the ice-cold NP-40 buffer just prior to adding it directly to the flask. For a T75cm^2 flask at 75% confluency, which is approximately 5x10^6 cells, 0.5 ml of NP-40 buffer was used. The pre-chilled rubber policeman was used to scrap the cells from the flask. The chilled NP-40 buffer, with the suspended cells, was transferred to a pre-cooled microcentrifuge tube. Samples were incubated for 30 minutes under a constant agitation, at 4^{o}C, followed by centrifugation for 20 minutes, at 12,000 rpm at 4^{o}C, then transferred to ice. The pellet was found to contain the proteins of interest. Lysate samples were stored at -80^{o}C.

Nuclear and Cytoplasmic Protein Extraction

To analyze the location of specific proteins in either the cytoplasm or the nucleus, a nuclear/cytoplasmic extraction was required. Following the NE-PER Nuclear and Cytoplasmic Extraction kit (Thermo Scientific, 78835), adherent cells were harvested with trypsin-EDTA and centrifuged for 5 minutes at 500 x *g.* Cells were washed in 1X PBS then 5 x 10^6 cells were transferred to a 1.5 ml microcentrifuge tube. The cells were pelleted by centrifugation at 500 x *g*

for 3 minutes and the supernatant was discarded, leaving the pellet as dry as possible. To the cell pellet, 500 µl of pre-chilled, ice-cold CER I buffer was added then vortexed vigorously until the cell pellet was fully suspended. The cell suspension was placed on ice to incubate for 10 minutes. After the incubation, 27.5 µl of pre-chilled, ice-cold CER II buffer was added to the cell suspension. Samples were vortexed for 5 seconds and placed on ice for 1 minute. Samples were vortexed again for an additional 5 seconds then were centrifuged for 5 minutes at 16,000 x *g.* The supernatant was immediately transferred into a pre-chilled 1.5 microcentrifuge tube. A 1 µl aliquot was taken from the supernatant and a small amount of the pellet was taken to the microscope to ensure purity of the extraction. The supernatant was stored as the cytoplasmic extracts. To the pellet, 500 µl of ice-cold NER buffer was added and samples were mixed vigorously by vortex for 15 seconds. The sample was placed on ice and was vortexed for 15 seconds every 10 minutes, for 40 total minutes. After the 40 minutes, samples were centrifuged for 10 minutes at 16,000 x *g.* The supernatant containing the nuclear extract was immediately transferred to a pre-chilled tube, analyzed under the microscope and stored at -80°C.

Western Blot Analysis

Protein analysis from whole cell, nuclear, and cytoplasmic extracts were performed through Western blot. In order to perform Western blot analysis, proteins were first separated by size through SDS-PAGE.

Protein Sample Preparation

Protein concentrations were determined before analysis through SDS-PAGE following the Pierce Assay (Thermo Scientific) protocol, using BSA dilutions to provide a standard curve. Protease inhibitor was added directly to 2X Laemmli buffer (0.125M Tris-HCl pH 6.8, 10% 2-mercaptoethanol, 20% glycerol, 0.0004% bromophenol blue, 4% SDS) prior to use. The 2X

Laemmli buffer was added at a 1:1 ratio to the cell lysate sample then boiled for 5 minutes. Any precipitation on the lid of the test tubes was collected by quick centrifugation.

SDS-PAGE

The BioRad mini-PROTEAN Tetra Cell was used to prepare and run all SDS-PAGE. A 6% Bis-acrylamide resolving gel (1.5M Tris-HCl, pH 8.8) and a 4% (0.5M Tris-HCl, pH 6.8) stacking gel were prepared for ideal separation for the proteins of interest. Gels were prepared according to the manufacturer's instructions (Invitrogen). When preparing the resolving gel, 10% APS and TEMED were added and gently swirled immediately before pouring between the two glass plates (approximately 4.5 ml). Double distilled water was then added directly on top of the monomer solution. After allowing the resolving gel to polymerize at room temperature for at least one hour, the water layer was removed and replaced with the 4% stacking gel with the addition of a 10 well comb. The stacking gel was allowed to polymerize for at least two hours before use.

Before loading the gel, the apparatus was filled with prepared Electrode (Running) Buffer (25 mM Tris-HCl, 192mM glycine, 0.1% SDS – pH 8.3; see recipes in Appendix). Prepared protein samples were loaded at a 30 µg final concentration, along with the BioRad molecular weight marker (Precision Plus Protein Dual Color Standard), which was run in parallel to the protein extracts. The gel was run at a constant 90V until the loading buffer reached the bottom of the resolving gel. Once electrophoresis was completed, the gel could be stained with Imperial Protein Stain (Pierce) overnight to analyze protein separation, or the gel was immediately used for Western blot analysis.

Western Blot

A semi-dry transfer method was used to transfer the proteins from the SDS-PAGE to a Polyvinylidene fluoride (PDVF) membrane (Millipore), to determine if the HT29 cell lysate contained the proteins of interest. The expression of the isoform B and myopodin was studied using an antibody provided by Dr. Chaolvich, at East Carolina University. The isoform B/myopodin specific antibody, denoted as NC_781, is a polyclonal antibody that was raised in rabbits against exon 4b (amino acid sequence: VWKPSVVEE) and affinity purified. The NC_781 antibody (3 mg/ml) was used at a 1:2,000 dilution. Beta-actin was used as a positive control (Sigma, A1978). A non-isoform specific synaptopodin-2 antibody was purchased from abcam (ab50192) to use as a comparison in expression patterns. Both secondary antibodies, goat anti-mouse (12-349) and goat anti-rabbit (12-348), were purchased from Millipore and were horseradish peroxidase conjugated. Aside from the NC_781 antibody, working dilutions were used at the manufacturer's recommendations.

To prepare for the protein transfer, the membrane and 3 mm whatman paper were cut to the dimensions of the gel. The gel was equilibrated in the continuous transfer buffer (39 mM Glycine, 48 mM Tris, 1.3 mM SDS, 20% Methanol – pH 9.2; see recipe in Appendix) while preparing the membrane. To prepare the membrane, it is placed in 100% methanol for 15 seconds, transferred to double distilled water for 2 minutes, then placed in the continuous transfer buffer for 5 minutes.Four pieces of pre-cut whatman paper, which have been soaked in the continuous transfer buffer, were placed on the anode electrode plate. The equilibrated membrane was transferred to the whatman paper; taking care to avoid any air bubbles from being formed between any of the layers. To help prevent the formation of air bubbles between the membrane and the gel layered just above it, a small amount of continuous transfer buffer was gently poured on the membrane before the gel was placed on top. An additional 4 pieces of whatman paper, soaked in the continuous transfer buffer, were placed on top of the gel. Any

excess transfer buffer was wiped off of the anode plate and the cathode plate was then placed on top and the transfer proceeded at 250mA for 40 minutes.

After the transfer, non-specific protein-protein interactions were blocked by incubating the membrane under constant agitation in 5% milk, diluted in TBST buffer (see recipe in Appendix), overnight at room temperature. After blocking, the membrane was washed 5 times at 5 minutes per wash with TBST and then incubated with the primary antibody (according to the previously mentioned dilutions) under constant agitation for 4 hours, at room temperature. The membrane is washed again with TBST (5 washes at 5 minutes per wash), and then incubated under constant agitation for 1 hour, at room temperature, with the secondary antibody. The membrane was thoroughly washed multiple times with TBST before proteins are visualized through chemiluminescence.

To visualize the proteins from the Western blot, chemiluminescence using Millipore substrate was performed. Chemiluminescent substrates for the horseradish peroxidase (HRP) are a two-component system, consisting of a stable peroxide solution and an enhanced luminol solution. To make a working solution of substrate, equal volumes of the two components (Millipore) were mixed together. The chemiluminescent working substrate was incubated on the membrane for 3 minutes, at room temperature. Excess substrate was removed from the membrane before exposure. A BioRad Universal Hood II light box with a Quantity One program was used to visualize proteins recognized by the primary antibody.

Cell Culture Transcription Inhibition

Actinomycin D (0.5 mg/ml) was used to treat HT29 cells to inhibit transcriptional activity. Cells were seeded at a density of $8x10^5$ on $18mm^2$ coverslips and allowed to adhere overnight in normal, complete DMEM/F12 media. The following day the normal media was removed and

cells were treated with complete DMEM/F12 media with Actinomycin D at a 1:1000 dilution. Control cells were incubated with 70% ethanol. Cells were left in the treatment media for 2, 4, and 8 hours before they were fixed and visualized following the protocol in the Immunocytochemistry section.

Cell Cycle Synchronization

HT29 cells were synchronized using Staurosporine (0.5 mg/ml; Millipore, 569397), Aphidicolin (10 mg/ml; Millipore, 178273), and Temozolomide (20 mg/ml; Sigma, T2577), which block the cell cycles in the G1 phase, S phase, and G2-M phase, respectively. To synchronize cells, $8x10^5$ cells were seeded on 18 mm^2 coverslips in normal, complete DMEM/F12 media and allowed to adhere overnight. The media was removed and replaced with complete DMEM/F12 media containing the specific inhibitor at a 1:1000 dilution. Cells were kept in treatment media for 24 and 36 hours. Control coverslips were treated with DMSO. The coverslips were used for immunocytochemistry to visualize cell cycle specific localization of isoform B/myopodin.

Immunocytochemistry

Immunocytochemistry was used to localize isoform B/myopodin within the cell structures. An asynchronous cell population, as well as cells blocked in specific phases of the cell cycle, were used to visualize protein localization within the cells. Cells were seeded on coverslips and allowed to adhere overnight. Cells were cultured to approximately 50% - 75% confluency. To fix cells on coverslips, the media was first removed and the coverslips were washed twice with PBS/Mg^{2+}, Ca^{2+}. Cells were fixed with 3.7% formalin in PBS/Mg^{2+}, Ca^{2+} for 8 minutes at room temperature. Cells were permeated with 0.1% Triton-X100 in 1X PBS at room temperature for 4 minutes. After a short rinse with 1X PBS, unspecific protein-protein

interactions were blocked with 10% FBS in 1X PBS for 45 minutes, at room temperature. The blocking solution was then removed and cells were incubated with the primary antibodies, diluted in 10% FBS/PBS, and incubated for 45 minutes. The coverslips were washed with 1X PBS 3 times for 10 minutes per wash and the cells were then incubated with the appropriate secondary antibody. Since the secondary antibodies are conjugated with a fluorescence dye, the coverslips were kept in the dark while incubating for an additional 45 minutes, at room temperature. The coverslips were kept in the dark to preserve their fluorescence for optimal visualization. After the final wash in 1X PBS the coverslips are mounted with Vectashield (Vector Laboratories, Inc.) and observed using an Olympus BX40 microscope. A QColor 5 Olympus camera and the QCapture Pro 6.0 program were used to generate cell pictures.

The NC_781 antibody was tittered out and a 1:600 dilution was established as the optimal working dilution. The synaptopodin-2 non-isoform specific Pan antibody (ab50192) and zyxin (ab58210) were purchased from abcam. The β-actin antibody (A1978) was purchased from Sigma, as well as the goat anti-rabbit (IgG, $F(ab)_2$ fragment-FITC) and the sheep anti-mouse (IgG, $F(ab)_2$ fragment-Cy3) secondary antibodies. A mouse anti-Nucleolin (39-6400) antibody was purchased from invitrogen. Purchased antibodies were used at the manufactures determined working concentration.

Antigen Competition Assay

To ensure that the expression pattern obtained through immunocytochemistry was the result NC_781 recognizing its appropriate epitope and not an artifact, a binding competition assay was performed. To do this, the minimal amount of antibody required to detect a fluorescence signal was first determined. A 1:1,200 dilution of the stock NC_781 antibody was the lowest concentration that yielded a detectable signal through immunofluorescence. Therefore a 1:1,200 was the final dilution factor used for the antibody. The NC_781 antibody

was incubated with the antigen amino acid sequence that processed the epitope (VWKPSVVEE) at different molar concentration ratios (antibody:antigen; 1:188, 1:150, 1:125) at room temperature for 4 hours under gentle but constant agitation. After the incubation, samples were centrifuged at 10,000 rpm at $4^{O}C$ for 30 minutes. The upper portion of the supernatant was collected and used as the primary antibody for immunocytochemistry. As a control, BSA was also incubated with the NC_781 antibody with the same molar concentrations as the antigen.

REFERENCES:

American Cancer Society (2020, Jun 29). Colorectal Cancer Stages. Web. 22 Jan 2021.

Andersen, J. S., Lam, Y. W., Leung, A. K., Ong, S. E., Lyon, C. E., Lamond, A. I., & Mann, M. (2005). Nucleolar proteome dynamics. Nature, 433(7021), 77–83. https://doi.org/10.1038/nature03207

Asanuma, K., Kim, K., Oh, J., Giardino, L., Chabanis, S., Faul, C., Reiser, J., Mundel, P. (2005). Synaptopodin regulates the actin-bundling activity of α-actinin in an isoform specific manner. J Clinical Investigation 155:1188-1198. https://doi.org/10.1172/JCI23371.

Augeron, C., & Laboisse, C. L. (1984). Emergence of permanently differentiated cell clones in a human colonic cancer cell line in culture after treatment with sodium butyrate. Cancer research, 44(9), 3961–3969.

Beall, B., & Chalovich, J. M. (2001). Fesselin, a synaptopodin-like protein, stimulates actin nucleation and polymerization. Biochemistry, 40(47), 14252–14259. https://doi.org/10.1021/bi011806u

Bevan, R., & Rutter, M. D. (2018). Colorectal Cancer Screening-Who, How, and When?. Clinical endoscopy, 51(1), 37–49. https://doi.org/10.5946/ce.2017.141

Boisvert, F. M., van Koningsbruggen, S., Navascués, J., & Lamond, A. I. (2007). The multifunctional nucleolus. Nature reviews. Molecular cell biology, 8(7), 574–585. https://doi.org/10.1038/nrm2184

Boulon, S., Westman, B. J., Hutten, S., Boisvert, F. M., & Lamond, A. I. (2010). The nucleolus under stress. Molecular cell, 40(2), 216–227.https://doi.org/10.1016/j.molcel.2010.09.024

Busch, H., Smetana, K. (1970). The Nucleolus. New York: Academic Press.

Beqqali, A., Monshouwer-Kloots, J., Monteiro, R., Welling, M., Bakkers, J., Ehler, E., Verkleij, A., Mummery, C., & Passier, R. (2010). CHAP is a newly identified Z-disc protein essential for heart and skeletal muscle function. Journal of cell science, 123(Pt 7), 1141–1150. https://doi.org/10.1242/jcs.063859

Castano, E., Philimonenko, V. V., Kahle, M., Fukalová, J., Kalendová, A., Yildirim, S., Dzijak, R., Dingová-Krásna, H., & Hozák, P. (2010). Actin complexes in the cell nucleus: new stones in an old field. Histochemistry and cell biology, 133(6), 607–626. https://doi.org/10.1007/s00418-010-0701-2

Cebrian, V., Alvarez, M., Aleman, A., Palou, J., Bellmunt, J., Gonzalez-Peramato, P., Cordón-Cardo, C., García, J., Piulats, J. M., & Sánchez-Carbayo, M. (2008). Discovery of myopodin methylation in bladder cancer. The Journal of pathology, 216(1), 111–119. https://doi.org/10.1002/path.2390

Chalovich, J. M., & Schroeter, M. M. (2010). Synaptopodin family of natively unfolded, actin binding proteins: physical properties and potential biological functions. Biophysical reviews, 2(4), 181–189. https://doi.org/10.1007/s12551-010-0040-5

Cho, R. J., Huang, M., Campbell, M. J., Dong, H., Steinmetz, L., Sapinoso, L., Hampton, G., Elledge, S. J., Davis, R. W., & Lockhart, D. J. (2001). Transcriptional regulation and function during the human cell cycle. Nature genetics, 27(1), 48–54. https://doi.org/10.1038/83751

Claeys, K. G., van der Ven, P. F., Behin, A., Stojkovic, T., Eymard, B., Dubourg, O., Laforêt, P., Faulkner, G., Richard, P., Vicart, P., Romero, N. B., Stoltenburg, G., Udd, B., Fardeau, M., Voit, T., & Fürst, D. O. (2009). Differential involvement of sarcomeric proteins in myofibrillar myopathies: a morphological and immunohistochemical study. Acta neuropathologica, 117(3), 293–307. https://doi.org/10.1007/s00401-008-0479-7

Cooper, G.M. (2000). The Eukaryotic Cell Cycle The Cell: A Molecular Approach. 2nd edition. Sunderland (MA): Sinauer Associates. Available from: https://www.ncbi.nlm.nih.gov/books/NBK9876/

De Ganck, A., De Corte, V., Staes, A., Gevaert, K., Vandekerckhove, J., & Gettemans, J. (2008). Multiple isoforms of the tumor suppressor myopodin are simultaneously transcribed in cancer cells. Biochemical and biophysical research communications, 370(2), 269–273. https://doi.org/10.1016/j.bbrc.2008.03.086

De Ganck, A., De Corte, V., Bruyneel, E., Bracke, M., Vandekerckhove, J., & Gettemans, J. (2009). Down-regulation of myopodin expression reduces invasion and motility of PC-3 prostate cancer cells. International journal of oncology, 34(5), 1403–1409.

Derenzini, M., Montanaro, L., & Treré, D. (2009). What the nucleolus says to a tumour pathologist. Histopathology, 54(6), 753–762. https://doi.org/10.1111/j.1365-2559.2008.03168.x

Derenzini, M., Montanaro, L., & Trerè, D. (2017). Ribosome biogenesis and cancer. Acta histochemica, 119(3), 190–197. https://doi.org/10.1016/j.acthis.2017.01.009

Donizy, P., Biecek, P., Halon, A., Maciejczyk, A., & Matkowski, R. (2017). Nucleoli cytomorphology in cutaneous melanoma cells - a new prognostic approach to an old concept. Diagnostic pathology, 12(1), 88. https://doi.org/10.1186/s13000-017-0675-7

Faul, C., Dhume, A., Schecter, A. D., & Mundel, P. (2007). Protein kinase A, Ca2+/calmodulin-dependent kinase II, and calcineurin regulate the intracellular trafficking of myopodin between the Z-disc and the nucleus of cardiac myocytes. Molecular and cellular biology, 27(23), 8215–8227. https://doi.org/10.1128/MCB.00950-07

Feng Z. (2010). p53 regulation of the IGF-1/AKT/mTOR pathways and the endosomal compartment. Cold Spring Harbor perspectives in biology, 2(2), a001057. https://doi.org/10.1101/cshperspect.a001057

Gao, J., Zhang, H. P., Sun, Y. H., Guo, W. Z., Li, J., Tang, H. W., Guo, D. F., Zhang, J. K., Shi, X. Y., Yu, D. S., Zhang, X. D., Wen, P. H., Shi, J. H., & Zhang, S. J. (2020). Synaptopodin-2 promotes hepatocellular carcinoma metastasis via calcineurin-induced nuclear-cytoplasmic translocation. Cancer letters, 482, 8–18. https://doi.org/10.1016/j.canlet.2020.04.005

Gilkes, D. M., Chen, L., & Chen, J. (2006). MDMX regulation of p53 response to ribosomal stress. The EMBO journal, 25(23), 5614–5625. https://doi.org/10.1038/sj.emboj.7601424

Guettler, S., Vartiainen, M. K., Miralles, F., Larijani, B., & Treisman, R. (2008). RPEL motifs link the serum response factor cofactor MAL but not myocardin to Rho signaling via actin binding. Molecular and cellular biology, 28(2), 732–742. https://doi.org/10.1128/MCB.01623-07

Hadjiolov, A. A. (1985). The Nucleolus and Ribosome Biogenesis. New York: SpringerVerlag.

Honda, K., Yamada, T., Endo, R., Ino, Y., Gotoh, M., Tsuda, H., Yamada, Y., Chiba, H., & Hirohashi, S. (1998). Actinin-4, a novel actin-bundling protein associated with cell motility and cancer invasion. The Journal of cell biology, 140(6), 1383–1393. https://doi.org/10.1083/jcb.140.6.1383

Jing, L., Liu, L., Yu, Y. P., Dhir, R., Acquafondada, M., Landsittel, D., Cieply, K., Wells, A., & Luo, J. H. (2004). Expression of myopodin induces suppression of tumor growth and metastasis. The American journal of pathology, 164(5), 1799–1806. https://doi.org/10.1016/S0002-9440(10)63738-8

Johnson, R. T., & Rao, P. N. (1970). Mammalian cell fusion: induction of premature chromosome condensation in interphase nuclei. Nature, 226(5247), 717–722. https://doi.org/10.1038/226717a0

Kai, F., Tanner, K., King, C., & Duncan, R. (2012). Myopodin isoforms alter the chemokinetic response of PC3 cells in response to different migration stimuli via differential effects on

Rho-ROCK signaling pathways. Carcinogenesis, 33(11), 2100–2107. https://doi.org/10.1093/carcin/bgs268

Kai, F., & Duncan, R. (2013). Prostate cancer cell migration induced by myopodin isoforms is associated with formation of morphologically and biochemically distinct actin networks. FASEB journal : official publication of the Federation of American Societies for Experimental Biology, 27(12), 5046–5058. https://doi.org/10.1096/fj.13-231571

Kai, F., Fawcett, J. P., & Duncan, R. (2015). Synaptopodin-2 induces assembly of peripheral actin bundles and immature focal adhesions to promote lamellipodia formation and prostate cancer cell migration. Oncotarget, 6(13), 11162–11174. https://doi.org/10.18632/oncotarget.3578

Khaymina, S. S., Kenney, J. M., Schroeter, M. M., & Chalovich, J. M. (2007). Fesselin is a natively unfolded protein. Journal of proteome research, 6(9), 3648–3654. https://doi.org/10.1021/pr070237v

Kołakowski, J., Wrzosek, A., & Dabrowska, R. (2004). Fesselin is a target protein for calmodulin in a calcium-dependent manner. Biochemical and biophysical research communications, 323(4), 1251–1256. https://doi.org/10.1016/j.bbrc.2004.08.224

Leinweber, B. D., Fredricksen, R. S., Hoffman, D. R., & Chalovich, J. M. (1999). Fesselin: a novel synaptopodin-like actin binding protein from muscle tissue. Journal of muscle research and cell motility, 20(5-6), 539–545. https://doi.org/10.1023/a:1005597306671

Lin, F., Yu, Y. P., Woods, J., Cieply, K., Gooding, B., Finkelstein, P., Dhir, R., Krill, D., Becich, M. J., Michalopoulos, G., Finkelstein, S., & Luo, J. H. (2001). Myopodin, a synaptopodin homologue, is frequently deleted in invasive prostate cancers. The American journal of pathology, 159(5), 1603–1612. https://doi.org/10.1016/S0002-9440(10)63006-4

Linnemann, A., van der Ven, P. F., Vakeel, P., Albinus, B., Simonis, D., Bendas, G., Schenk, J. A., Micheel, B., Kley, R. A., & Fürst, D. O. (2010). The sarcomeric Z-disc component myopodin is a multiadapter protein that interacts with filamin and alpha-actinin. European journal of cell biology, 89(9), 681–692. https://doi.org/10.1016/j.ejcb.2010.04.004

Liu, J., Ye, L., Li, Q., Wu, X., Wang, B., Ouyang, Y., Yuan, Z., Li, J., & Lin, C. (2018). Synaptopodin-2 suppresses metastasis of triple-negative breast cancer via inhibition of YAP/TAZ activity. The Journal of pathology, 244(1), 71–83. https://doi.org/10.1002/path.4995

Lodish, H., Berk, A., Zipursky, S.L. (2000). The Dynamics of Actin Assembly. Molecular Cell Biology. 4th edition. New York: W. H. Freeman; 2000. Section 18.2, Available from: https://www.ncbi.nlm.nih.gov/books/NBK21594/

Mundel, P., Heid, H. W., Mundel, T. M., Krüger, M., Reiser, J., & Kriz, W. (1997). Synaptopodin: an actin-associated protein in telencephalic dendrites and renal podocytes. The Journal of cell biology, 139(1), 193–204. https://doi.org/10.1083/jcb.139.1.193

Pham, M., & Chalovich, J. M. (2006). Smooth muscle alpha-actinin binds tightly to fesselin and attenuates its activity toward actin polymerization. Journal of muscle research and cell motility, 27(1), 45–51. https://doi.org/10.1007/s10974-005-9053-2

Pompas-Veganzones, N., Sandonis, V., Perez-Lanzac, A., Beltran, M., Beardo, P., Juárez, A., Vazquez, F., Cozar, J. M., Alvarez-Ossorio, J. L., & Sanchez-Carbayo, M. (2016). Myopodin methylation is a prognostic biomarker and predicts antiangiogenic response in advanced kidney cancer. Tumour biology : the journal of the International Society for Oncodevelopmental Biology and Medicine, 37(10), 14301–14310. https://doi.org/10.1007/s13277-016-5267-8

Qi, W., Li, J., Pei, X., Ke, Y., Bu, Q., & Ni, X. (2020). β-Actin facilitates etoposide-induced p53 nuclear import. Journal of biosciences, 45, 34.

Raska, I., Koberna, K., Malínský, J., Fidlerová, H., & Masata, M. (2004). The nucleolus and transcription of ribosomal genes. Biology of the cell, 96(8), 579–594. https://doi.org/10.1016/j.biolcel.2004.04.015

Renfranz, P. J., & Beckerle, M. C. (2002). Doing (F/L)PPPPs: EVH1 domains and their proline-rich partners in cell polarity and migration. Current opinion in cell biology, 14(1), 88–103. https://doi.org/10.1016/s0955-0674(01)00299-x

Rubbi, C. P., & Milner, J. (2003). Disruption of the nucleolus mediates stabilization of p53 in response to DNA damage and other stresses. The EMBO journal, 22(22), 6068–6077. https://doi.org/10.1093/emboj/cdg579

Sanchez-Carbayo, M., Schwarz, K., Charytonowicz, Cordon-Cardo, C., Mundel, P. (2003). Tumor suppressor role for myopodin in bladder cancer: loss of nuclear expression of myopodin is cell-cycle dependent and predicts clinical outcome. Oncogene 22, 5298–5305. https://doi.org/10.1038/sj.onc.1206616

Schroeter, M., & Chalovich, J. M. (2004). Ca2+-calmodulin regulates fesselin-induced actin polymerization. Biochemistry, 43(43), 13875–13882. https://doi.org/10.1021/bi0487490

Schroeter, M. M., Beall, B., Heid, H. W., & Chalovich, J. M. (2008). The actin binding protein, fesselin, is a member of the synaptopodin family. Biochemical and biophysical research communications, 371(3), 582–586. https://doi.org/10.1016/j.bbrc.2008.04.134

Schroeter, M. M., Orlova, A., Egelman, E. H., Beall, B., & Chalovich, J. M. (2013). Organization of F-actin by Fesselin (avian smooth muscle synaptopodin 2). Biochemistry, 52(29), 4955–4961. https://doi.org/10.1021/bi4005254

Shen, X., Valencia, C. A., Szostak, J. W., Dong, B., & Liu, R. (2005). Scanning the human proteome for calmodulin-binding proteins. Proceedings of the National Academy of Sciences of the United States of America, 102(17), 5969–5974. https://doi.org/10.1073/pnas.0407928102

Siegel, R. L., Miller, K. D., Goding Sauer, A., Fedewa, S. A., Butterly, L. F., Anderson, J. C., Cercek, A., Smith, R. A., & Jemal, A. (2020). Colorectal cancer statistics, 2020. CA: a cancer journal for clinicians, 70(3), 145–164. https://doi.org/10.3322/caac.21601

Tsai, R. Y., & McKay, R. D. (2002). A nucleolar mechanism controlling cell proliferation in stem cells and cancer cells. Genes & development, 16(23), 2991–3003. https://doi.org/10.1101/gad.55671

Towbin, H., Staehelin, T., & Gordon, J. (1979). Electrophoretic transfer of proteins from polyacrylamide gels to nitrocellulose sheets: procedure and some applications. Proceedings of the National Academy of Sciences of the United States of America, 76(9), 4350–4354. https://doi.org/10.1073/pnas.76.9.4350

Van Impe, K., De Corte, V., Eichinger, L., Bruyneel, E., Mareel, M., Vandekerckhove, J., & Gettemans, J. (2003). The Nucleo-cytoplasmic actin-binding protein CapG lacks a nuclear export sequence present in structurally related proteins. The Journal of biological chemistry, 278(20), 17945–17952. https://doi.org/10.1074/jbc.M209946200

Weins, A., Schwarz, K., Faul, C., Barisoni, L., Linke, W. A., & Mundel, P. (2001). Differentiation- and stress-dependent nuclear cytoplasmic redistribution of myopodin, a novel actin-bundling protein. The Journal of cell biology, 155(3), 393–404. https://doi.org/10.1083/jcb.200012039

White R. J. (2005). RNA polymerases I and III, growth control and cancer. Nature reviews. Molecular cell biology, 6(1), 69–78. https://doi.org/10.1038/nrm1551

Xia, E., Zhou, X., Bhandari, A., Zhang, X., & Wang, O. (2018). Synaptopodin-2 plays an important role in the metastasis of breast cancer via PI3K/Akt/mTOR pathway. Cancer management and research, 10, 1575–1583. https://doi.org/10.2147/CMAR.S162670

Yuan, X., Zhou, Y., Casanova, E., Chai, M., Kiss, E., Gröne, H. J., Schütz, G., & Grummt, I. (2005). Genetic inactivation of the transcription factor TIF-IA leads to nucleolar disruption, cell cycle arrest, and p53-mediated apoptosis. Molecular cell, 19(1), 77–87. https://doi.org/10.1016/j.molcel.2005.05.023

Yu, Y. P., & Luo, J. H. (2006). Myopodin-mediated suppression of prostate cancer cell migration involves interaction with zyxin. Cancer research, 66(15), 7414–7419. https://doi.org/10.1158/0008-5472.CAN-06-0227

Zylber, E. A., & Penman, S. (1971). Products of RNA polymerases in HeLa cell nuclei. Proceedings of the National Academy of Sciences of the United States of America, 68(11), 2861–2865. https://doi.org/10.1073/pnas.68.11.2861

APPENDIX

Appendix A: Tables

Table 1: Primer Sequences for individual Synaptopodin-2 Isoforms

Primer name	Sequence (5' to 3')	Annealing Temperatures	Product Size
Synpo2 variant 1F	ATCAGCCTCATCATCTTATTTTGT	59 °C	251 bp
Synpo2 variant 1R	CCACTAGACCGAGAGGAGACTTTG		
Synpo2 variant 2F	AAAGCAAGAATCAGCCTCATCATC	66 °C	192 bp
Synpo2 variant 2R	GCTAGGCATTCTCAGGGACTCAAG		
Synpo2 variant 3F	TCCCACCTCGCCAAAGCAAGAAT	59 °C	252 bp
Synpo2 variant 3R	GGAGCCCAAGAAATAGGAGATGTG		

Table 1: RT-PCR primer sequences for the individual synaptopodin-2 isoforms. The appropriate annealing temperatures and product lengths for the individual isoforms are indicated.

Table 2: Primer Sequences for Isoform B and Myopodin Full-Length Gene PCR Amplification

Primer name	Sequence (5' to 3')	Annealing Temperatures	Product Size
Synpo2StartF	GAGAAGCTTAAAACATGGGCACAGGGGATTTTATCTGC	60°C	
Myopodin Forward	GAGAAGCTTAAAACATGTTTAAGAAGCGACGTCGGAGG	60°C	2136 bp
RevComp Synpo2B	GAGGGATCCTTAGTGATGGTGATGGTGATGGCCCCCTCCCTCTTCCACAACAGATGGTTTCC	60°C	3282 bp

Table 2: Primer sequences for full length gene amplification of synaptopodin-2 Isoform B and myopodin. The appropriate annealing temperature and expected product length is indicated.

Table 3: SDS-Gel Recipe

Percent Gel	DDI H2O (ml)	40% Degassed Acrylamide/Bis (ml)	Gel Buffer* (ml)	10% (w/v) SDS (ml)
4%	6.4	1	2.5	0.1
6%	5.9	1.5	2.5	0.1

Table 7: Recipe for making different concentrations of SDS-polyacrylamide gels. Bis-acrylamide was purchased through BioRad. Resolving *Gel Buffer- 1.5M Tris-HCl, pH 8.8; *Stacking Gel Buffer- 0.5M Tris-HCl, pH 6.8. For resolving gels add 50 µl 10% APS and 5 µl TEMED and for stacking gels add 50 µl 10% APS and 10 µl TEMED

Appendix B- Recipes

- **10 % (w/v) SDS**
  - 10 g of SDS in 90 ml of water. Stir gently and bring the total volume to 100 ml with double distilled water.

- **1.5 M Tris-HCl, pH 8.8**
  - 27.23 g of Tris base (18.15 g/100 ml) and add 80 ml of double distilled water. Adjust pH to 8.8 with 6N HCl. Bring total volume to 150 ml with double distilled water and store at 4^{o}C.

- **0.5 M Tris-HCl, pH 6.8**
  - 6 g Tris base and add 60 ml of double distilled water. Adjust pH with 6N HCl and bring total volume to 100 ml with double distilled water. Store at 4^{o}C.

- **10X Electrode (Running) Buffer, pH 8.3**
  - 30.3 g Tris base
  - 144.0 g glycine
  - 10.0 g SDS
  - Dissolve and bring the total volume to 1,000 ml with double distilled water. The buffer solution was stored at 4^{o}C. If precipitation occurred, the buffer was warmed to room temperature before use.

- **10 % (w/v) APS**
  - Dissolve 100 mg of ammonium persulfate in 1 ml of double distilled water. Store at 4^{o}C up to one week.

- **50X TAE Stock Solution (For preparing and running PCR gels)**
  - 242g Tris Base (MW= 121.1g/mol), 57.1 ml Glacial Acetic Acid, 100 ml 0.5M EDTA. Bring to the final volume of 1 L with ddH_2O.

- **Continuous Transfer Buffer**
  - 2.93g Glycine
  - 5.82g Tris base
  - 0.0375g SDS
  - 200ml Methanol
  - Dissolve and bring the total volume to 1,000 ml with double distilled water. The buffer solution was stored at 4^{o}C.

- **Tris-buffered Saline (TBS) 10X**
  - 24.23 g Trizma HCl
  - 80.06 g NaCl
  - pH to 7.6 with pure HCl
  - Dissolve and bring the total volume to 1,000 ml with double distilled water.

- **Tris-buffered saline with Tween20 (TBST) 1X**
  - 100ml TBS 10X
  - 900ml double distilled water
  - 1ml Tween20

- **Phosphate-buffered Saline (PBS) 10X**
  - NaCl 80g
  - KCl 2g
  - KH2PO4 2g
  - Na2HPO4 11.3g
  - Dissolve and bring the total volume to 1,000 ml with double distilled water.

- **PBS/$Mg^{2+,}$ Ca^{2+} 1X**
  - 5 ml of 100 mM MgCl2
  - 9 ml of 100 mM CaCl2
  - 100 ml of 10X PBS
  - Dissolve and bring the total volume to 1,000 ml with double distilled water.